Nanoscale Advances

ROYAL SOCIETY OF CHEMISTRY

REVIEW

View Article Online
View Journal | View Issue

Cite this: *Nanoscale Adv.*, 2021, **3**, 4321

Self-assembly in biobased nanocomposites for multifunctionality and improved performance

Emily Olson,[ab] Fei Liu,[a] Jonathan Blisko,[c] Yifan Li,[a] Ayuna Tsyrenova,[a] Rebecca Mort,[ab] Keith Vorst,[bd] Greg Curtzwiler,[bd] Xin Yong *[c] and Shan Jiang *[ab]

Concerns of petroleum dependence and environmental pollution prompt an urgent need for new sustainable approaches in developing polymeric products. Biobased polymers provide a potential solution, and biobased nanocomposites further enhance the performance and functionality of biobased polymers. Here we summarize the unique challenges and review recent progress in this field with an emphasis on self-assembly of inorganic nanoparticles. The conventional wisdom is to fully disperse nanoparticles in the polymer matrix to optimize the performance. However, self-assembly of the nanoparticles into clusters, networks, and layered structures provides an opportunity to address performance challenges and create new functionality in biobased polymers. We introduce basic assembly principles through both blending and *in situ* synthesis, and identify key technologies that benefit from the nanoparticle assembly in the polymer matrix. The fundamental forces and biobased polymer conformations are discussed in detail to correlate the nanoscale interactions and morphology with the macroscale properties. Different types of nanoparticles, their assembly structures and corresponding applications are surveyed. Through this review we hope to inspire the community to consider utilizing self-assembly to elevate functionality and performance of biobased materials. Development in this area sets the foundation for a new era of designing sustainable polymers in many applications including packaging, construction chemicals, adhesives, foams, coatings, personal care products, and advanced manufacturing.

Received 27th May 2021
Accepted 26th June 2021

DOI: 10.1039/d1na00391g

rsc.li/nanoscale-advances

1. Introduction

Petrochemical based plastics are widely used due to their low cost and robust mechanical properties.[1,2] However, petroleum based plastics are not sustainable. In addition, impurities and mixtures prohibit effective recycling, all raising concerns of environmental pollution. On the other hand, biobased polymers such as cellulose, starch, chitosan, polylactic acid (PLA) and their derivatives, have been studied for many years. Early development of polymers already demonstrated the great potential of biobased plastics. For example, modified cellulose derivatives Parkesine and celluloid were initially invented in the mid-1800s to help address the ivory crisis, and later successfully developed into many different products.[3] Henry Ford experimented with soy protein as a replacement material for the metal parts of automobiles.[4] George Washington Carver introduced peanut protein to derive biobased plastics.[5] History has already shown that one potential approach to address the petroleum plastic challenge is to replace it with biobased polymers.[6–8]

Compared with conventional petroleum-based polymers, there are some major features generally associated with biobased polymers: (1) diverse chemical composition and heterogeneous structures even for the same type of biobased materials; (2) prevalent amount of hydrogen bonds; (3) difficulty in processing; (4) relatively high cost; (5) lack of mechanical performance and functionality. Correspondingly, these also represent key challenges when broad application of biobased materials is attempted. Even for the same materials, variable sources result in different molecular weight, chain conformations, degree of modification, and chirality.[9–11] Furthermore, many biobased polymers including starch and cellulose, have predominant amounts of hydrogen bonds, which are susceptible to water swelling and penetration. These materials are more prone to degrade and have narrow processing window and poor temperature stability. For example, processing is especially challenging for PLA with a melting temperature of ~160 °C and degradation temperature starting at 200 °C. In addition, biobased polymers are generally more expensive than petrochemical polymers, largely due to limited availability and high raw material cost. Aside from price, biobased polymers are also

[a]*Mateirals Science and Engineering, Iowa State University, Ames, IA 50011, USA. E-mail: sjiang1@iastate.edu*

[b]*Polymer and Food Protection Consortium, Iowa State University, Ames, IA 50011, USA*

[c]*Mechanical Engineering, Binghamton University, Binghamton, NY 13902, USA. E-mail: xyong@binghamton.edu*

[d]*Food Science and Human Nutrition, Iowa State University, Ames, IA 50011, USA*

limited by their performance. Furthermore, biobased materials oftentimes have issues in mechanical strength and environmental stability.[12] To match the conventionally desired properties of petrochemical plastics, significant improvement of biobased polymers is required.

Self-assembled hierarchical structures have been demonstrated to enhance the benefit of the nanoparticle and even introduce new capabilities.[13–15] However, the majority of attention in nanocomposite development has been directed to petroleum polymers, whose chain conformations and modifications are better controlled and understood compared to their biobased counterparts.[16] A plethora of nanoparticle structures have been demonstrated in petrochemical polymer systems: dispersions[17–41] and films,[42–47] as well as assembly structures of clusters,[48–50] chains,[51–57] and networks.[58–62] In addition, simply mixing nanoparticles in biobased polymer matrices have been reviewed,[63–67] though mainly in the areas of bioderived fillers (*i.e.* cellulose) and clays.[9,68,69] One major challenge in nanocomposite formulation is to disperse the nanoparticles and prevent aggregation. It is known that random aggregation occurs due to high surface area, high surface energy, and strong inter-particle attractions. These factors lead to random aggregates with lower Gibb's free energy, which is detrimental to material performance.[70–73] Controlling the spatial distribution and assembly of nanoparticles relies on a delicate balance of intermolecular forces, between nanoparticles and with the polymer matrix.[74,75] To ultimately disperse the nanoparticles, enthalpy driven thermodynamic miscibility must be achieved.[76] The hydrogen bonding capacity of biobased polymers provides a foundation for dispersion. High shear can also be used for dispersion, though stability afterwards depends highly on thermodynamics and the ability of the particles to stay in kinetically trapped states. Dispersed nanoparticles may then assemble into more complex structures such as clusters and networks, introducing new opportunities to elevate composite properties (Fig. 1). For example, pre-composite polymers have been demonstrated to encapsulate titanium dioxide nanoparticles for spatially separated nanoparticles for improved opacity of coatings.[77] In addition, strategically designed self-assembly offers a tool to create novel functionality and expand the application of biobased polymers, including water resistance, light modulating, conductivity, antibacterial and corrosion resistance.[78,79] Since assembly structures of nanocellulose in biobased matrices have been extensively reviewed, the topic will not be repeated in this report.[80,81] Instead, the focus here is on the more recent development of hierarchical self-assembly of inorganic nanoparticles in biobased polymer matrix. It is critical to recognize the challenges associated with the complexities in polymer chemistry and lack of fundamental understanding of interactions.

Interactions amongst nanoparticles and with surrounding matrix is the key to understand assembly structures in nanocomposites. All the fundamental forces, including van der Waals force, electrostatic force, steric hindrance and hydrophobic force, should be considered in nanocomposite design. These interactions have already been thoroughly investigated in petroleum-based polymers.[82,83] However, biobased polymers

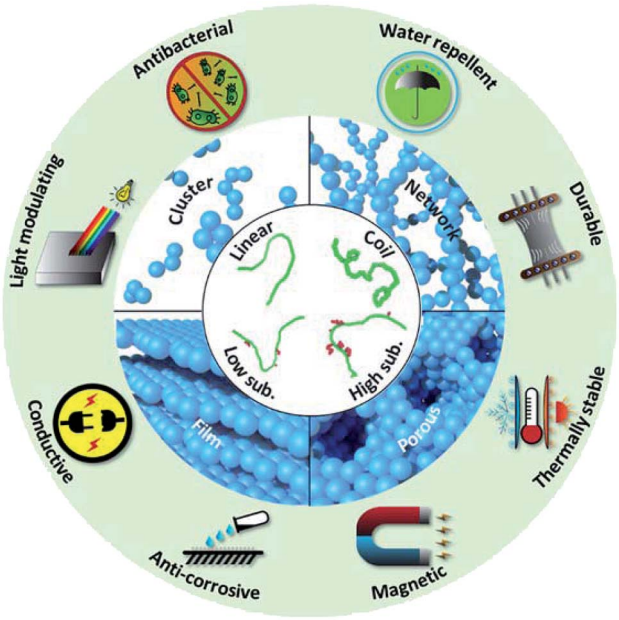

Fig. 1 Schematic chart of structures involved in biobased nanocomposite and possible enhanced properties offered by nanoparticle assembly.

also have their own unique interactions, due to the prevalence of hydrogen bonding, and their three-dimensional structures. Biobased polymers can further induce other interactions such as depletion force, capillary force, and bridging interactions. All of the aforementioned forces are related to the size, chain architecture and morphology, which present a rather complicated scenario.[84]

Biobased nanocomposites have been formed *via* two major techniques: blending and *in situ* synthesis. In blending, the nanoparticle and polymer are simply mixed *via* solvent or melt compounding. Solvent mixing reduces viscosity to facilitate material transport.[85] In melt compounding, the polymer chains diffuse into the space between the nanoparticles. Extrusion is often utilized to enhance the efficiency and economic viability of this approach.[86] A key challenge in both solvent mixing and melt compounding methods is the prevention of random nanoparticle aggregation, which can hurt the performance of the nanocomposite.[87,88] This is especially problematic in melt compounding, where viscosity is elevated.[86] Aggregation may be prevented through surface modification or reducing the nanoparticle concentration. Alternatively, *in situ* synthesis can be used to avoid the need to mechanically disperse the nanoparticles, as the particles themselves are synthesized *in situ* within the polymer matrix.[89] With the polymer acting as the template, capping agent or both, this method promotes good spatial distribution of the synthesized particles in a single step. However, the *in situ* assembly method has certain limitations. Since particle synthesis and assembly occur in a single step, controlling assembly is much more challenging.[90]

This review covers the fundamental interactions at molecular level, structure–property relationships, and the end applications of assembly structures in biobased nanocomposites

(Fig. 1). We first discuss the morphology considerations of the biobased polymer matrix. Next, we identify different types of nanoparticle assembly structures, including cluster, network, alignment, porous structures, and multilayer films. Subsequently, key assembly mechanisms and intermolecular forces are addressed. We then highlight new functionality imparted to the composite by nanoparticle assembly and discuss the relationships between assembly and functionality. Computational simulation is a powerful tool that can be used to compliment experimental approaches. However, currently there are very few simulation studies that showcase nanoparticle self-assembly in biobased polymers,[91,92] due to largely variable and complicated chemistry of biobased polymers.[93] A brief survey of the progress is included. It is important to consider the safety issue when applying nanoparticles in biobased matrix. Specific safety metrics vary widely depending on the specific application (food packaging, cosmetics, personal and home care, *etc.*). Safety consideration will also be different as to whether nanoparticles would be released from matrix during usage or by the end of life of the product. However, discussing this topic at length is out of the scope of this manuscript. This review will help set the foundation and offer guidance for future work in designing biobased nanocomposite materials for novel functionality and enhanced performance.

2. Polymer conformation

A deep understanding of interactions and structure–property relationships is critical in the design of biobased composite systems. A key challenge in biobased materials is their many (and often complicated) chain conformations. The chirality, the architecture, the persistence length and chain morphology can all vary drastically even for the same type of biobased material. This is due to a number of factors including source material, extraction method and post-treatment approach.[94–96] Starch, for example, often takes on a helical conformation with laterally oriented chains. Based on the source (rice, potato, corn *etc.*), amylose and amylopectin presentation can vary. Starch chains are majorly composed of amylopectin, with average unit chain sizes ranging from 20–25. Several chain distributions of amylopectin exist, all of which vary in chain length and degree of branching.[97,98] Amylose, is the minor component, and is composed of linear chains that varying in size from four to more than one hundred units. Slight branching is again possible, depending on the source material.[99] For example, it has been shown that maize and smooth pea starch are more branched than wrinkled pea and potato.[100] Source material (and the resulted amylose and amylopectin ratio/composition) can also impact the hydrogen bonding of water to exposed hydroxyl groups of amylose and amylopectin, modifying the swelling and solubility profile. Potato starch, for example, has a 56 times larger swelling capacity than that of purple yams.[101]

Though almost identical in chemical composition for the repeating monomeric unit, cellulose takes on a very different conformation at the expense of its *trans* glycosidic linkage. There are numerous polymorphs to consider, from native (I) to processed native cellulose (II–VI). Cellulose chains can widely vary in polymerization as a result of the source material. For example wood cellulose has a degree of polymerization of ~10 000, while cotton cellulose has a degree of ~15 000.[102] With increasing length, the chains become more rigid and apt to form hydrogen bonds within the chain (as observed in crystals).[103] It is possible for these rod-like structures to form clusters and even sheets. Modified cellulose (such as hydroxyethyl and hydroxypropyl) have been demonstrated to form fringed micelles, whose structures can vary drastically depending on chain length and flexibility.[11]

Diverse chain conformations have also been observed in lignin, chitosan, and PLA. Lignin, a side product of cellulose forms cross-linked phenolic structures, which can be both aromatic or aliphatic.[104] Chitosan, a biopolymer found in marine exoskeletons, is composed of randomly mixed β-(1,4) linked *N*-acetylglucosamine and glucosamine units.[105] The chain morphology can vary dramatically with temperature and pH, allowing rod, globule, and coil conformations.[106] The commercialized biobased polymer PLA is biodegradable polyesters synthesized through bioderived monomers lactic acid or 2-hydroxy propionic acid. The polymer may take on D(−) or L(+) stereoisomer conformations which determine crystallinity, glass transition, and melting temperature.[107]

Key differences in biobased polymer sourcing induce disparities in the chain conformation and degree of substitution, which makes quality control and industrialization efforts difficult. The polymer matrix largely determines the shape, structure, and function of the material, and composition variation introduces difficulties in consistent material performance. Therefore, it is important to keep the chain confirmation in mind when studying nanocomposites. With the introduction of nanoparticles, the polymer matrix determines the assembly structures and modulates the performance, enhancing existing properties and offering new functionality.

3. Nanoparticles for performance and functionality

Water resistance in biobased materials has significant room for improvement. The prevalence of hydroxy groups on the polymer backbone imparts a strong affinity to water molecules, which is particularly problematic for applications such as food packaging and coatings, where water vapor can induce degradation and bacterial growth. With nanoparticle assembly, together with chemical surface treatments, biobased polymers can help render surface hydrophobic. For example, silica dioxide (SiO_2) particles can introduce water resistance to thermoplastic starch (with lycopodium spores) and isosorbide epoxy resin through post salinization.[108,109] Zinc oxide (ZnO),[110,111] titanium dioxide (TiO_2),[112,113] and clay[114] have been demonstrated to improve the hydrophobicity of conventionally hydrophilic polymers including chitosan, epoxy, starch, and alginate. In addition, nanoparticles can even render the surface less vapor permeable, largely due to the tortuous paths introduced by the nanoparticles.

In the same regard, nanoparticles can be added to address challenges between toughness and stiffness of biobased

Table 1 Nanocomposite formulation and property summary

Nanoparticle	Biobased materials	Fabrication	Structure	Key properties	References
TiO_2	Cellulose, chitosan, starch, PLA, whey protein	*In situ* (polymer template and capping agent), blending (solvent)	Dispersion, cluster, network, film	Durable, water repellent, light modulating, thermally stable	15, 112, 113 and 145–154
ZnO	Cellulose, chitosan, starch, PLA, polyhydroxybutyrate	*In situ* (capping agent), blending (solvent)	Dispersion, cluster, network, film	Durable, water repellent, light modulating, thermally stable, antibacterial	93, 110, 111, 124, 155–168
SiO_2	Cellulose, starch, PLA, whey protein, soy protein	*In situ* (polymer template and capping agent), blending (solvent and melt)	Dispersion, cluster, network, film	Durable, water repellent, thermally stable	34, 108, 109, 169–177
GO	Cellulose, chitosan	Blending (solvent)	Dispersion, film	Durable, water repellent, thermally stable	178 and 179
Au	Cellulose, chitosan, starch	*In situ* (polymer template and capping agent), blending (solvent)	Dispersion, network	Light modulating, conductive	180–187
Ag	Cellulose, chitosan, lignin, polylactide, alginate	*In situ* (polymer template and capping agent), blending (solvent)	Dispersion, cluster, network, film	Water repellent, light modulating, antibacterial	14, 119–122, 130–144, 185, 187–197
Fe_3O_4	Cellulose, starch	*In situ* (polymer template and capping agent), blending (solvent)	Dispersion, cluster	Durable, light modulating, thermally stable, conductive, magnetic	123, 198–201
Clay	Cellulose, chitosan, starch, PLA	Blending (solvent and melt)	Cluster, film	Durable, water repellent, light modulating, thermally stable	114, 125, 126, 202–208

composites. The mechanical character of the composite depends on both the inherent properties of the nanoparticle and polymer matrix, though assembly structure and interfacial contact distribution are large contributors to durability. Cellulose nanoparticles have been widely used for this purpose in a number of matrices including PLA,[115] chitosan, starch, and gelatin matrices.[116,117] Since cellulose nanoparticles have already been thoroughly reviewed, here we will focus on inorganic nanoparticles.[118] Following, silver,[119] silica,[120] and clay[121,122] have been demonstrated to impart enhanced robustness to the biobased polymer matrix.

Nanoparticles can also aid in introducing additional functionalities such as corrosion resistance and antibacterial activity. Corrosion is a key challenge in composites subject to weathering. Biobased epoxy is commonly utilized for corrosion resistance due to its durability, toughness, and adhesion to metal surfaces. Diverse nanoparticle identities have been demonstrated for anticorrosion, filling the interstitial spaces of the polymer insulator and preventing ion penetration at the coating–metal interface. A variety of nanoparticles including Fe_3O_4,[123] ZnO,[124] clay,[125,126] silica,[109] and carbon nanotubes[127–129] have been utilized for anticorrosive applications. In addition, nanoparticles have been widely reported in the introduction of antibacterial activity. The antibacterial efficacy of silver has been well studied and has found a great number of applications because of its relatively low toxicity. Silver has been shown to introduce antibacterial properties to a number of biobased materials including gelatin,[130,131] cellulose,[132,133] starch,[134–138] and chitosan.[139–142] Silver nanoparticles have also been synthesized on the surface of other nanoparticle compositions for antibacterial improvement.[143,144] Magnetic, conductive, light modulating, and thermal stability can also be imparted to biobased composites by nanoparticles (Table 1).

4. Fundamentals of nanoparticle assembly in biobased polymers

Self-assembly into hierarchical structures such as networks and clusters opens new opportunities to further enhance biobased polymer properties. The end performance of the nanocomposite is dependent on the collective performance of the assembly, and specific attention must be given to interparticle interactions and structure–property relationships.[209] A number of key interactions are relevant in the discussion of how nanoparticles assemble. Hydrogen bonding, specifically, has been demonstrated as a determining factor in nanoparticle assembly

formation in biobased matrices. Bioderived materials, such as starch and cellulose, have glycosidic backbones that are rich in hydroxyl groups. These groups largely participate in hydrogen bonding. Hydrogen bonding is a relatively strong, short range force.[210,211] The orientation of the formed bonds is directly dependent on the donor and acceptor geometries.[72,84] These characteristics of hydrogen bonding play an important role in encouraging thermodynamic miscibility, which provides the foundation to assemble nanoparticles into unique structures.

Hydrophobic interactions are another key force in the formation of biobased nanocomposite assemblies. The origin of hydrophobic forces are related to the lack of hydrogen bonding of water with hydrophobic surfaces, though the range and magnitude of hydrophobic force is still under debate.[84,212] Hydrophobic interactions are prevalent for many non-polar entities and responsible for their aggregation in the presence of aqueous medium.[84] Actually protein utilized the hydrophobic collapse to fold into specific 3-D conformations. Therefore, geometric placement of hydrophobic moieties may also assist the assembly of nanoparticles. Other forces have also been demonstrated to play a role in nanoparticle assembly, for example, van der Waals (vdW) force. The origin of vdW force is created by the transient dipole moment when electron orbiting nucleus, therefore it is a universal attractive force. Although the vdW force is relatively weaker than hydrogen bonding and short ranged,[213] integration over all the atoms and molecules on nanoparticles may produce significant overall amount of attraction when nanoparticles become very close to each other.[214] vdW force only directly impacts nanostructure formation below a certain distance threshold, and may help lock the arrangement of nanoparticles in place once assembly is achieved.[84]

Beyond the fundamental forces, there are other forces more specifically related to polymer morphology in the assembly process. One such force is bridging, where the polymer absorbs on the particle surface, hence connecting it to other particles to form larger assembly structures.[215,216] In the case that the polymer does not adsorb on the polymer surface, depletion is possible when distance between nanoparticles is smaller than the radius of gyration of the polymer. The depletion force is strong and occurs at a relatively long (nm–μm) onset distance.[217] In moderate to dilute cases, depletion has an entropic origin that arises from the steric repulsion between polymers and the particle surface. The proximity between particles establishes exclusion zones, which induce concentration gradients of polymers. The resulted osmotic pressure leads to solvent movement and the attraction of neighboring particles to form aggregates.[218–220] Increased entropy allows the polymers to freely diffuse in newly available volume. All of the aforementioned intermolecular forces are variable in degree and onset distance (Fig. 2). Thermodynamic and kinetic contributions should both be considered in self-assembly processes. Thermodynamics contributes to the establishment of systematic equilibrium, which may alter the ultimate assembly state of particles for the long term. Kinetics may temporarily determine assembly structures, which is directly impacted by processing and assembly conditions.

Assembly can be tuned *via* control of surface modifications of nanoparticles, molecular weight of biobased polymers, and restriction of film thickness. Assembly structures can be organized into two categories: clusters and networks. In the scope of this review, the term 'cluster' refers to local particle aggregation. A 'network' is an interconnected, percolated structure which may or may not be porous. Films (single and multilayer) will also be addressed in this report. Although a 'film' is a compact stacking of particles which covers the entire substrate surface, they are often formed through assembled clusters. Experimentally, nanoparticles are dispersed in polymer matrices through two major methods, *in situ* synthesis and blending. First, *in situ* synthesis of nanoparticles within the polymer matrix will be discussed. The method boasts several advantages, such as thorough particle dispersion and controllable particle size and geometry. However, there are few reports of complex assembly structures.[90] The second method addressed in this review is blending. Blending includes both melt compounding and solvent mixing. Blending is advantageous economically, though to prevent random aggregation, introduction of additives such as surfactants is often needed. Beyond the experimental approach, computational simulations have been demonstrated as a versatile and straightforward route toward identifying interfacial interactions and even future design for optimized nanocomposite (and self-assembly).[216] Theoretical modelling of

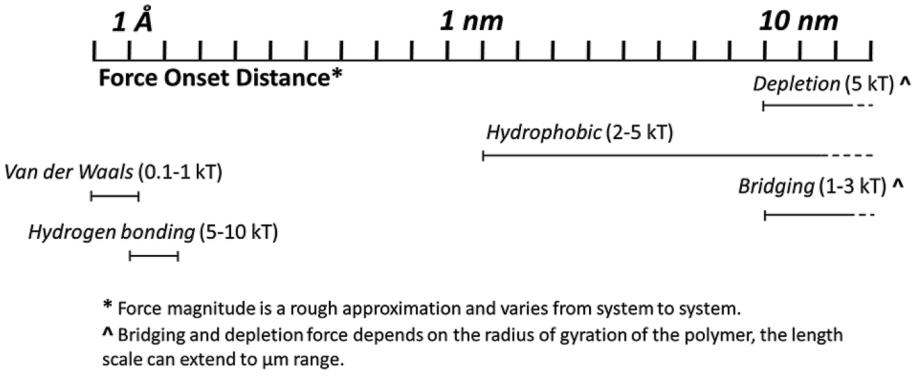

Fig. 2 Strength of the polymer induced forces which mediate nanoparticle assembly into hierarchical structures. *Distances are only rough approximations, and magnitudes vary from system to system.

both *in situ* and blending approaches is a powerful technique to predict and validate experimental data. However, the reports in this area are relatively limited. In surveying simulated and experimental nanoparticle self-assembly, we showcase current progress in the biobased material development and identify challenges for future research directions.

5. Nanoparticle synthesis *in situ* in biobased matrices

A key challenge in the formulation of biobased nanocomposites is ensuring that the nanoparticle is homogenously dispersed. *Ex situ* methods, which involve blending of polymers and previously synthesized nanoparticles, see difficulty with random aggregation.[89] An attractive approach to disperse the nanoparticles is the *in situ* synthesis of nanoparticles within the polymer matrix *via* sol–gel chemistry or hydrothermal/solvothermal methods. Nanoparticle synthesis *in situ* requires the use of a monomer/precursor, such as a metal salt, and a reducing agent, both in a nonreactive solvent.[221] Following synthesis, the nanoparticles are assembled, with both processes occurring in one-pot. This approach initiates unique assembly structures and enhanced control of particle geometry, size, and initial aggregation. However, the post-synthesis assembly is difficult to control, and synthetic methods must be designed carefully to optimize assembly and the resulting nanocomposite functionality. In this section, we summarize the *in situ* synthesis and assembly of inorganic nanoparticles in biobased matrices using template and external field.

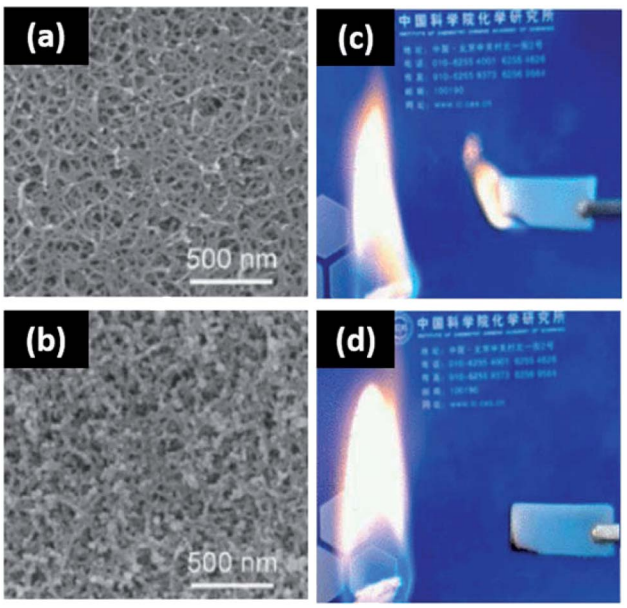

Fig. 3 Templated assembly of silica nanoparticles *via* CO_2 drying for flame retardancy. (a) SEM micrograph of cellulose-only aerogel; (b) SEM micrograph of cellulose–silica composite aerogel; (c) flame repellency of the cellulose-only aerogel; (d) cellulose-templated silica aerogel. This figure has been adapted from ref. 221 with permission from the American Chemical Society, 2017.

5.1 Oxide nanoparticles

One of the most commonly used nanoparticles in coating and composite technology is titanium dioxide. Titanium dioxide has a high refractive index, making it a particularly effective opacifier. However, TiO_2 is known to form random aggregates at the expense of its surface chemistry, and this process has been shown to deteriorate its light blocking properties. Therefore, *in situ* nanoparticle synthesis is an attractive method to control the aggregation of TiO_2 nanoparticles in polymeric composite systems. Miao *et al.* synthesized TiO_2 nanoparticles in cellulose matrices with 1-allyl-3-methylimidazolium chloride ionic liquid.[145] Through this approach, the nanoparticles were assembled into a film with variable pore size. Gupta, *et al.* synthesized TiO_2 *via* electro spraying with spun PLA fibers to form a film.[148] TiO_2 nanoparticles have been synthesized *via* sol–gel methods as well, with regenerated cellulose[149] and chitosan as the polymer scaffolds.[150]

Supercritical CO_2 drying, magnetic field ordering, and silica condensation have been demonstrated in the synthesis of silica nanoparticle assemblies *in situ*. Yuan *et al.* used regenerated cellulose gel as a template to formulate silica composite aerogels *via* a sol–gel process with supercritical CO_2 drying to attain

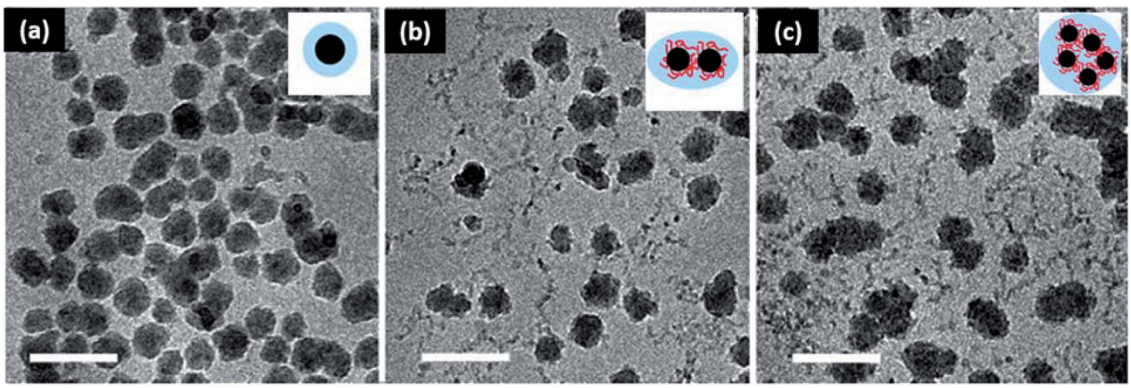

Fig. 4 Silica cluster formation with hydroxyethyl cellulose loading for drug delivery applications. (a) 0.1% w/v, (b) 0.5% w/v, and (c) 1% w/v hydroxyethyl cellulose. Scale bar is 100 nm. This figure has been adapted from ref. 176 with permission from the Royal Society of Chemistry, 2018.

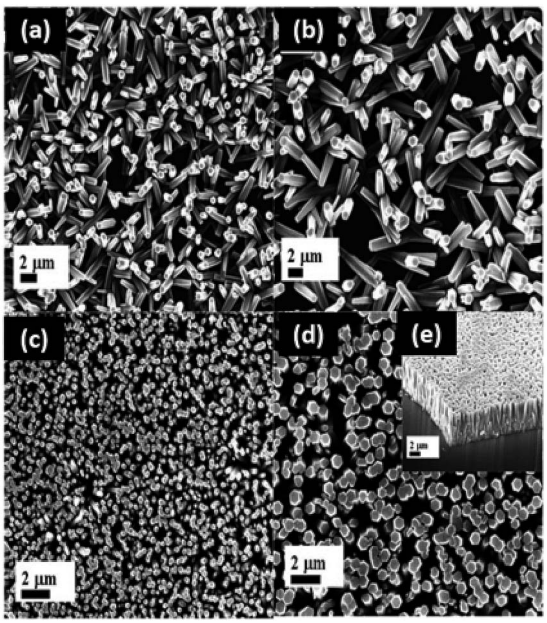

Fig. 5 ZnO nanorod alignments at high nanoparticle loading (3.5, 7.5 mg mL^{-1}) for optoelectronic devices. At lower concentrations (<3.5 mg mL^{-1}), the nanorods grow in random directions. Cellulose–ZnO solutions containing 3.5 mg mL^{-1} of cellulose concentration with (a) 0; (b) 1.0; (c) 3.5; (d) 7.5 mg mL^{-1} of ZnO nanoparticles; and (e) cross section image of ZnO nanorods alignment with 7.5 mg mL^{-1} ZnO. This figure has been adapted from ref. 162 with permission from MDPI, 2013.

a porous network (Fig. 3).[222] The silica sol entered the cellulose gel network, filling the voids in the substrate without aggregation. It was found that the incorporation of silica enhanced the specific surface area and mesoporous characteristic of the cellulose template. The barrier formed by silica decreased the rate of cellulose decomposition, enhancing flame retardancy. The same method with nanocrystalline cellulose can produce chiral nematic assemblies of silica from liquid crystal nanocellulose ordering.[223] Network structures of silica can also be mediated by local ordering with a magnetic field.[176] Less complex silica clusters can be synthesized *via* self-condensation of 3-mercaptopropyltrimethoxysilane in the presence of hydroxyethyl cellulose. Interestingly, polymer concentration directly controls cluster size, with increased loading enhancing bridging interactions and yielding larger clusters (Fig. 4).[177]

Another highly common inorganic nanoparticle in forming nanocomposite materials is zinc oxide. ZnO boasts impressive ultraviolet light protection and antibacterial activity.[143,167] Like titanium dioxide, random aggregation can be detrimental to these functionalities.[165] A number of studies synthesized ZnO nanoparticles *in situ*, with the biobased polymers serving as both scaffolds and stabilizing agents. Vigneshwaran *et al.* synthesized dispersed ZnO particles in an aqueous system of soluble starch, which served as both the stabilizer and size controlling agent.[158] Synthesis *in situ* is also useful in designing complex particle geometries. In fact, Carp *et al.* used starch to synthesize single phase donut shaped zinc oxide. The starch acts as both a stabilizer and template in this study, allowing for the formation of homogenous ZnO spheres, which upon heating converted to donut morphologies.[159] Other cluster structures such as flowers have also been synthesized *in situ*.[160]

More complex assemblies of ZnO such as networks and alignments can provide property enhancement to biobased polymer matrices. In the formation of network assemblies, the polymer matrix can serve as both the stabilizing and flocculating agent. Networks have been reported in carboxymethyl starch[161] and cellulose[166] matrices. In the same regard, polymers can align zinc oxide nanoparticles. Ibupoto *et al.* hydrothermally synthesized films of aligned ZnO nanorods with starch or cellulose as the seed initiator.[163] It was shown that the polymer identity and concentration was essential in determining the nanorod alignment (Fig. 5). A similar study was conducted by Zhao and coworkers for antibacterial efficacy.[224] The ZnO nanoparticles were demonstrated to grow *in situ* along cellulose nanofibers, which align into mats. ZnO microparticles grow between the mats of cellulose and ZnO nanoparticles to form a multi-layered structure.

5.2 Metallic nanoparticles

Metallic nanoparticles such as silver, gold, platinum, and copper have been prevalently synthesized *via in situ* methods.[225] These nanoparticles are known to aggregate due to their large Hamaker constant,[84] and in some applications (electrical,

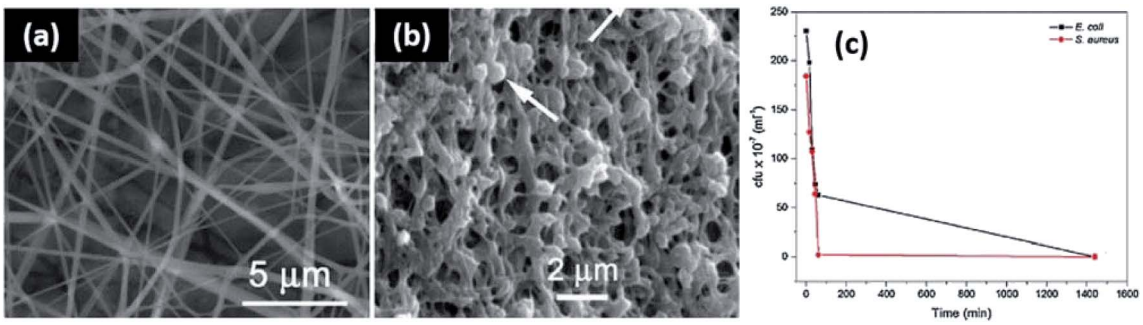

Fig. 6 Porous structure of silver–chitosan film complexes on porous alginate templates for antibacterial efficacy. (a) SEM micrograph of bare alginate fibers; (b) SEM micrograph of alginate fibers post immersion in a chitosan–silver nanoparticle solution; (c) antibacterial activity against *E. coli* and *S. aureus*. This figure was adapted from ref. 189 with permission from Elsevier, 2017.

medical, *etc.*), cluster size and particle geometry require deliberate control. If assembled carefully, metallic nanocomposites can serve as lightweight electrical and sensitive magnetic materials.[226] Synthesis *in situ* can help limit random aggregation and is particularly beneficial in these applications. For example, Shankar *et al.* used lignin as the reducing agent for the formulation of dispersed silver nanoparticles in PLA.[193] Additional size and dispersity control are provided with the application of microwave and ultraviolet irradiation. Hu *et al.* achieved homogenously nucleated silver particles with starch, amino acids, and microwave heating.[14] The nanoparticles demonstrated assembly into films, with applications as Raman spectroscopy sensors. Ultraviolet irradiation can serve to expedite the reduction of silver ions to nanoparticles upon excitation of their polymeric matrix. Basuny *et al.* used carboxymethyl cellulose with ultraviolet irradiation to achieve thoroughly dispersed silver nanoparticles.[196]

Film structures have also been reported with metallic particles *in situ*. For example, Mokhena *et al.* formed silver nanoparticles *in situ* with chitosan, and then deposited on a template of electro spun alginate fibers to produce films with enhanced antimicrobial activity.[190] In both cases of Gram positive and negative bacteria, no growth was observed after 24 hours. This is largely a result of the porous assembly structure, which aids in water absorption and silver nanoparticle release into the media. Post immersion, the alginate retained its structure, with the Ag clusters embedded between the chitosan and alginate layers as a film (Fig. 6). Chitosan was also used with cellulose micro fibrils to promote silver film formation.[197] Silver films have been identified with lignin and starch as well.[227,228]

Gold nanoparticles have been synthesized *in situ* with thermoresponsive poly(*N*-isopropylacrylamide) for plasmonic applications.[229] Chitosan has also been reported as a reducing agent in the synthesis of gold *in situ*. When combined with poly(L-lysine), chitosan can serve as the reducing, capping, and stabilizing agent in the *in situ* synthesis of gold nanoparticle clusters.[230] The addition of different organic acids (acetic, malonic, oxalic) can be applied to tune the reduction rate and particle morphology.[182] Gold nanoparticle geometry can also be controlled with starch in the presence of ultrasonic waves[184] and ionic liquids on cellulose templates.[181] Complex network structures of silver, gold, platinum, and copper can be synthesized *via* cellulose nanocrystal templating and cetyltrimethylammonium bromide stabilization.[185] Iron oxide nanoparticles can be synthesized *via* similar *in situ* methodologies to those observed in metallic nanoparticles. Gholoobi *et al.* used starch to control the size and aggregation of Fe_3O_4 nanoparticles.[198] Polymer templates such as cellulose nanocrystals[200] and microporous regenerated cellulose have also been reported in iron oxide nanoparticle synthesis.[201]

We have shown here that largely diverse nanoparticle identities (ceramic, metal, *etc.*) can be synthesized *via in situ* methods with biobased polymers. The polymers can behave as the capping agent, template, or both. *In situ* syntheses present new opportunities for tunable particle size, geometry, and aggregation, however, complex assemblies are not reported often.[90] Intricate assembly structures are addressed more thoroughly in reports of simple nanoparticle–polymer blending, which will be the core focus of this review.

6. Assembly *via* nanoparticle blending in biobased matrices

Blending is the simplest approach to formulate biobased nanocomposites. Here, pre-synthesized nanoparticles are combined with biobased polymers (and other additives) *via* solvent mixing or melt compounding. Since the particles are not being synthesized within the polymer matrix as they were with *in situ* methods, thorough dispersion is required prior to polymer addition. Nanoparticles are prone to form random aggregates due to their high surface energy, therefore understanding and mediating interactions between particles and the environment is of critical importance. Inorganic nanoparticle films and assemblies (clusters and networks) have been reported *via*

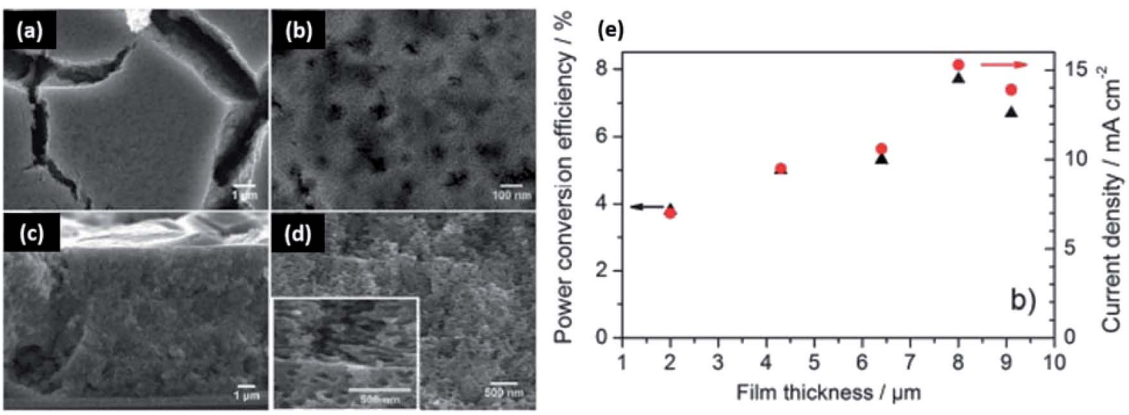

Fig. 7 Porous structures of titanium dioxide in ethyl cellulose matrices with Pluronic 127 surfactant for power conversion. SEM micrographs of (a) film morphology prior to calcination, (b) film morphology after calcination, (c) cross-section before calcination, (d) cross-section after calcination, and (e) the optoelectronic properties as a function of film thickness. This figure was adapted from ref. 151 with permission from Elsevier, 2014.

Table 2 Comparison of the light blocking properties of TiO_2 nanocomposites with differing polymer matrices and resulted assembly structures

Polymer matrix	Film thickness (um)	Assembly structure	%Transmittance (300 nm)	%Transmittance (600 nm)
Whey protein[151]	50	Cluster	0	2
Potato starch[147]	80	Dispersion	0	4
Wheat starch[146]	120	Cluster	0	10
Hydroxyethyl cellulose[165]	0.2	Network	0	20
Polyaniline chitosan[15]	1.5	Film	17	70

blending processing techniques. When compared with *in situ* synthesis, the blending technique has the advantage of simplicity and flexibility, with a simple setup and the possibility of using commercially available nanoparticles, which usually leads to lower cost and less effort in preparation. Therefore, blending presents an economical method in the application of biobased polymer technologies.

6.1 Oxide nanoparticles

6.1.1 Titanium dioxide

6.1.1.1 Clusters and networks. Titanium dioxide (TiO_2) nanoparticles are commonly used in the fields of composites and coatings due to their opacifying properties. In most cases fully dispersed particles are desired, as large aggregates are detrimental to composite performance.[77] However, literature suggests that carefully controlled structures of titania can introduce novel capabilities to the biobased nanocomposite. For example, Goudarzi *et al.* demonstrated that TiO_2 nanoparticle clusters in starch matrices promote enhanced hydrophobicity and UV-blocking.[146] The clusters form from hydrogen bonding interactions with starch, and decrease the water solubility. The clusters are shown to introduce roughness to the composite, which offers additional contribution to improving the water contact angle. The coating has been suggested for use in packaging for UV-blocking applications. Clusters of TiO_2 nanoparticles may also be utilized for an anti-plasticizing effect. In a whey protein matrix, Zhou *et al.* used cluster size to control the tensile and moisture barrier properties.[151] Small amounts of nanoparticle were shown to improve the tensile strength, but hydrophobicity was reduced. The opposite phenomena were observed with larger quantities. The decreased strength at high loading occurs due to increased cluster size, which creates discontinuities in the polymer domains.

Dense network structures of titania have also been demonstrated in the formulation of materials for smart windows and dye solar cells.[231,232] In this scenario, biobased polymers assist in viscosity modulation for the formulation of uniform colloidal pastes. Ethyl cellulose is commonly used as a thickener to achieve viscous screen printable pastes when the fabrication process of TiO_2 electrode involves the use of organic solvent-based formulations.[233,234] Biobased polymer matrices can also aid in enhancing surface porosity after removing organics *via* sintering. The resulting film is composed of interconnected mesoporous TiO_2 networks, where the desired thickness can be achieved by repetitive coating.[233] Feckl *et al.* formed mesoporous films of TiO_2 in ethyl cellulose with Pluronic F127 surfactant.[152] The bimodal assembly exhibits small (6–8 nm) pores from the surfactant and large pores (60–100 nm) from the ethyl cellulose (Fig. 7). The films are light scattering and increasing thickness increases the power conversion efficiency. Chen *et al.* achieved a crack-free nanostructured TiO_2 film using methyl cellulose as a binder in an aqueous formulation.[235] It has been shown that adding hydroxyethyl cellulose to a polymeric gel leads to the nanostructured and porous morphology of TiO_2 film with a large surface area. Prepared dye solar cells exhibited higher power conversion and photovoltaic performance compared to the electrodes made with a conventional paste, emphasizing the importance of assembly in material property determination.[236]

6.1.1.2 Films. Polymer choice can provide control in the formation of nanoparticle assembly structures from simple clusters to complex multilayer films. The structures may provide enhanced functionality to the polymer matrix. Take TiO_2 nanoparticles as an example, the key property of TiO_2 is to improve light blocking capacity in both the ultraviolet and visible range. The opacifying properties of the TiO_2 nanocomposite films presented in this section are summarized (with coating thickness) in Table 2. Clearly, different polymer matrices can be utilized in the formation of assembly structures varying in complexity. Small scale assembly structures such as clusters promote the best light blocking in the ultraviolet and visible range. Though network and films are not the most effective opacifying structures, in this section we showcase functionalities unique to higher level assemblies such as dye degradation, hydrophobicity, power conversion, and flame retardancy.

Deposition of TiO_2 as a coating film has been demonstrated to provide dramatic property enhancement to the polymer substrate. For example, Lu *et al.* synthesized films of cellulose and TiO_2 (modified with 1*H*,1*H*,2*H*,2*H*-perfluoroalkyltriethoxysilane) as a low surface energy coating for wood.[153] Scanning electron microscopy images show that the TiO_2 coating does not change the cellulose structure, instead filling the pits between fibers. Increasing water resistance was achieved with more layers, and pH was also shown to be a key factor. When pH was increased, charges on polymer were altered and more effective depositions and hydrophobicity were achieved. Environmental stability tests showed maintained properties for a number of days. Gilman *et al.* formulated multilayer coatings on cotton *via* the same method using chitosan.[237] Cotton fabrics were submerged in the polymer–nanotube suspension repeatedly. It was shown that the nanotubes

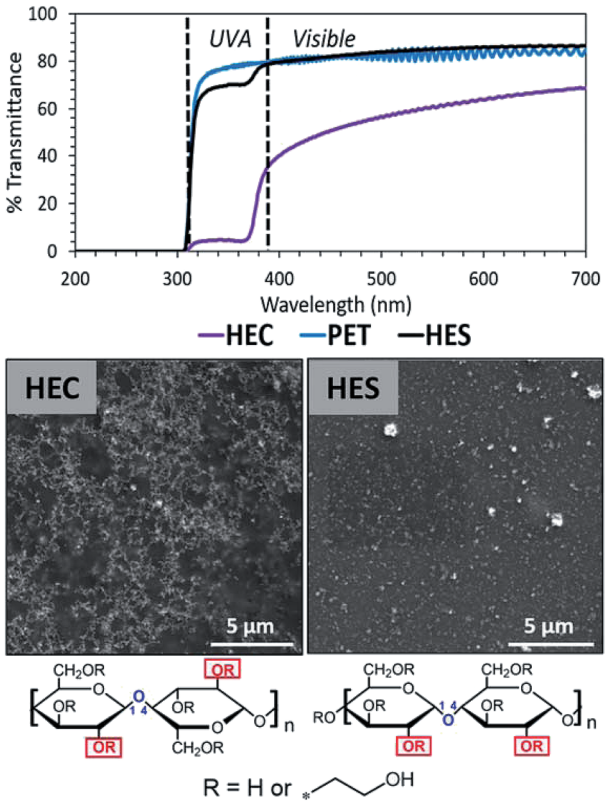

Fig. 8 Cluster and network structures of zinc oxide nanoparticles in hydroxyethyl starch and hydroxyethyl cellulose matrices. Only network structures promote UV-blocking. This figure has been adapted from ref. 164 with permission from ACS Publications, 2019.

assembled in a random and entangled fashion, and modification of the number of layers and the polymer particle-ratio provides additional structural control. The network formed is shown to induce thermal stability, providing a barrier to heat, oxygen, and mass transfers when the fabric is exposed to a flame. Inclusion of TiO_2 nanoparticles reduces gas transport *via* tortuous pathways, and their radical scavenging capability encourages stable char formation, hence preventing cotton surface regeneration for combustion.

Multilayer coatings of TiO_2 can be formed through electrostatic interactions. Mahanta *et al.* used polyaniline grafted chitosan as a positive electrolyte to bridge multilayer percolated films.[15] The films are effective in promoting the degradation of anionic and cationic dyes, with grafted chitosan driving the dye towards TiO_2 for degradation. Interestingly, the films can be reused for this purpose, which emphasizes the stability and utility offered by multilayer coating structures.

6.1.2 Zinc oxide

6.1.2.1 Clusters and networks. Like TiO_2, zinc oxide (ZnO) also boasts high levels of ultraviolet light absorption. It is prevalently used in cosmetics and packaging industries to protect light sensitive items including the human epidermis, foods, and dyes. Nanoparticle assembly structures of ZnO, such as clusters and networks, have been reported to impart impressive light blocking properties to biobased polymers.[162,165] For example, Olson *et al.* formulated network structures of ZnO in hydroxyethyl cellulose matrices for a high UV-blocking (95%) performance.[165] In comparison, hydroxyethyl starch formed a dispersion of clusters, not a network, under the same formulation conditions (Fig. 8). This occurs as a result of configuration of the anomeric bonds. The α-anomer in the starch derivative yields a coiled structure with lower persistence length, and the β-anomer of cellulose increases the persistence length and polymer rigidity. This variation has drastic impacts on the resulted nanoparticle assemblies and UV-blocking capacity.

Networks of ZnO nanoparticles have also been demonstrated in regenerated cellulose matrices by Fu *et al.*[162] Enhanced nanoparticle loading was found to induce the formation of increasingly interconnected clusters structures in the composite. The structures were firmly embedded in the polymer matrix, likely due to strong hydrogen bonding interactions between polymer and particle. These interactions enhanced the tensile strength and Young's modulus of the composite. The films also displayed UV-blocking properties (99%) and impressive antibacterial activities against *E. coli* and *S. aureus*.

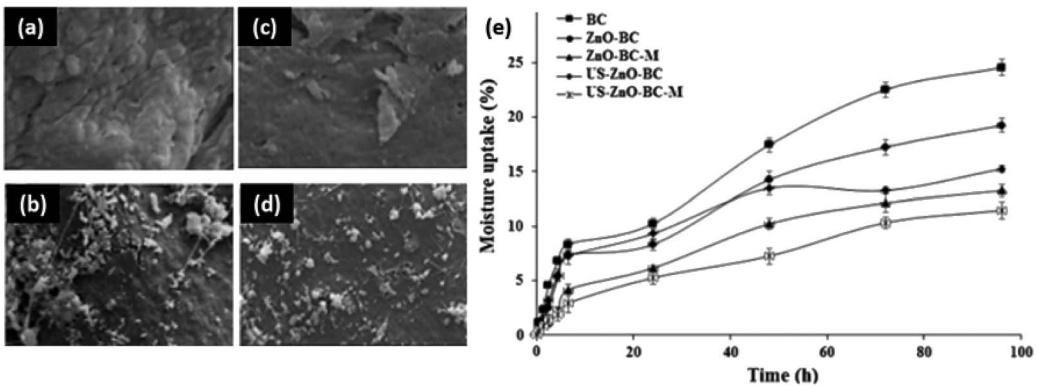

Fig. 9 Ultrasonication techniques in the formation of zinc oxide networks in bacterial cellulose for water repellency. SEM images of (a) bacterial cellulose, (b) bacterial cellulose with ZnO, (c) multilayer bacterial cellulose with ZnO, (d) bacterial cellulose with ZnO processed *via* ultrasonication, (e) moisture uptake comparison. This figure has been adapted from ref. 167 with permission from Elsevier, 2020.

6.1.2.2 Films. When ZnO nanoparticles are deposited as a film, enhanced antibacterial activity and water repellency are reported. Valerini *et al.* formulated a monolayer of aluminum doped ZnO nanoparticle on PLA films *via* a sputtering technique.[167] The deposition power greatly altered the nanoparticle structure on the PLA surface. With low deposition power, the surface of the polymer is filled with particle, leading to a smooth appearance. Increasing deposition power increases the roughness and surface coverage. The roughness offered by larger deposition power significantly improve the hydrophobicity of the coating. As in previous studies, the coating also shows antibacterial activity.

Films can be assembled together to form multiple layers, introducing diverse functionality to the substrate. Particle identity and layer ordering are key in determining the final properties of the coating. Bacterial cellulose and ZnO porous multilayer sandwich structures have been reported by Jebel *et al.*[168] Ultra-sonication was used to control nanoparticle aggregation, reducing cluster size and allowing for their effective (entangled) interactions with the cellulose fibers. Without ultra-sonication, the nanoparticles were solely absorbed on the fiber surface (Fig. 9). The strong interaction between cellulose and ZnO is a result of hydrogen bonding, and with the addition of ultra-sonication the water vapor permeability and moisture absorption is improved dramatically. The films were again shown to be antibacterial against *S. aureus* and *E. coli*, an effect enhanced by ultrasonication.

6.1.3 Silica dioxide

6.1.3.1 Clusters and networks. Silica dioxide (SiO_2) nanoparticles have been demonstrated to enhance the microstructure and mechanical performance of polymeric materials.[238] In the nanocomposite, silica nanoparticles introduce matrices of higher densities, imparting strength, improved thermal properties, and durability under working conditions.[238] The incorporation of SiO_2 nanoparticles in biobased polymers have been extensively studied to improve the coating performance.[169,174,175] Nanostructures of silica ranging in complexity have been reported by Ai *et al.* in soy protein matrices *via* compression molding.[175] As the nanoparticle loading increases, nanoclusters, interconnected networks, and large domains are possible. The formation of network nanostructures is shown to alter the strong, interfacially ordered soy protein matrix, eventually leading to micro phase domain separation. The inherent strength of the composite is dictated by the polymer–filler interface, and therefore stronger prior to micro domain formation, with aggregation severely limiting elongation capacity. Superhydrophobic network structures of SiO_2 nanoparticles were achieved by Olson *et al. via* solvent mixing in hydroxyethyl cellulose.[239] The rigid chain conformation of hydroxyethyl cellulose was utilized to strategically form flocculated silica nanoparticle assemblies at multiple length scales. Hydroxyethyl starch only formed dispersions of small clusters of nanoparticles. Furthermore, when the composite was treated with fluorinated silane vapor, superhydrophobicity was achieved with cellulose. It is proposed that the roughness of nanoparticle assembly in cellulose is responsible for the superhydrophobic property (Fig. 10). The composite is also self-cleaning and promotes impressive adhesion.

Network structures of silica were also formed by Saxena *et al.* in the presence of sodium carboxymethyl cellulose, cetyltrimethylammonium bromide (CTAB), and oxalic acid.[173] Due to limitations induced by the coffee ring effect, SiO_2 nanoparticles cannot organize into such complex structures alone. With the electrostatic and surface tension effects of CTAB and the crystallization ability of oxalic acid, homogenous fractal structures can take shape *via* van der Waals forces. Interestingly, these structures can be utilized for improved hydrophilicity and antifogging properties. Network structures of silica were also demonstrated by Zhang *et al.* with the use of starch sponges as the polymer template.[240] Pore size and network density is found to be highly dependent on starch concentration. The silica frameworks could be removed (and kept intact) *via* calcination. The films are highly robust and resist degradation in a number of solvents including water and acetone.

6.1.3.2 Films. The added benefit of silica nanoparticles has been reported in film structures. In one method by Pinto *et al.*, films of SiO_2 were assembled layer-by-layer with cellulose and polyelectrolytes.[172] Adhesion of the particles to the cellulose fibers is determined by electrostatic interactions between the particles and polyelectrolyte. For means of comparison, particles were also formed *via in situ* synthesis. Interestingly, the *in situ* approach resulted in denser coatings, likely due to precursor condensation during growth. This study demonstrates the importance of synthesis strategy in dictating

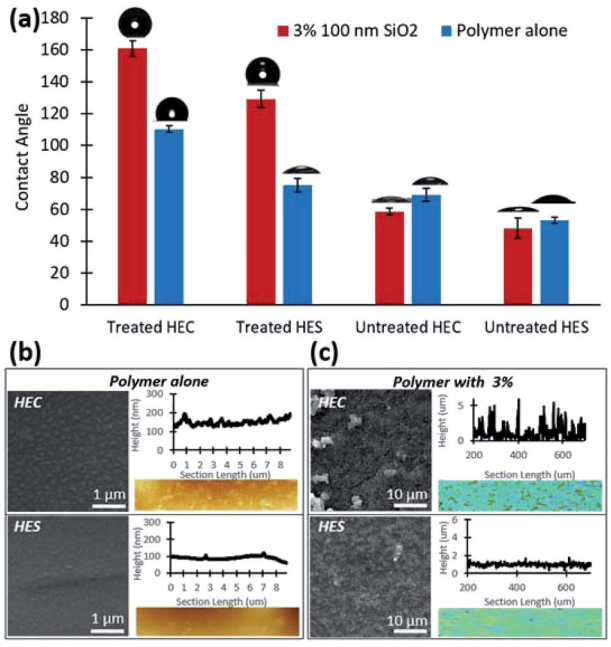

Fig. 10 Polymer mediated network and cluster assemblies of silica in hydroxyethyl cellulose and starch matrices for water repellency. (a) Contact angle as a function of polymer, nanoparticle, and surface treatment; (b) SEM micrographs of fluoro silane treated composites of HEC and HES alone with an AFM topography profile; (c) SEM micrographs of silane treated HEC and HES nanocomposites with a confocal topography profile. This figure has been adapted from ref. 238 with permission from the Royal Society of Chemistry, 2021.

nanoparticle assembly and composite properties. In both scenarios, water uptake is reduced compared to the bare cellulose fibers.

6.1.4 Clay

6.1.4.1 Clusters and networks. Clay is a mineral composed of small crystals of silica and aluminum oxide, along with traces of organic materials. Like SiO_2, clay too offers improved mechanical strength and barrier properties to biobased nanocomposites. Therefore, clay is oftentimes used for food packaging applications.[241,242] Liu *et al.* reported clusters of clay in nanocomposites of cellulose nanofibers modified with protonated chitosan.[202] Chitosan provides hydrophilicity and its charge helps disperse the filler. When added, the chitosan intercalates amongst clay layers, causing immediate flocculation. The dry coating is homogenous and smooth, with strength provided by cellulose nanofibers and clay (up to 48% loading). Clay has also been demonstrated to assemble into clusters *via* solvent mixing with carbon nanotubes in chitosan.[243] Tang *et al.* observed the nanotubes to surround the clay platelets, reinforcing the chitosan matrix. Increasing nanoparticle content initiated the formation of clay clusters, improving the thermal stability, strength, and gas permeability of chitosan. The composite is suggested for use in food packaging applications. Yoon *et al.* used raw corn starch to form clusters of kaolin clay *via* precipitation with ammonium sulfate.[203] It was shown that starch effectively coats clay platelets, and increased loading induces the formation of clusters. Cluster diameter is found to determine composite strength, water solubility, and opacity. These properties can be achieved with small quantities of clay, allowing for dramatic composite performance improvement without strength sacrifice.

Network structures of clay have also been reported in biobased polymer matrices. Low molecular weight poly(-vinylalcohol) (PVOH) was used in the melt compounding of chitosan–clay nanocomposites by Giannakas *et al.*[244] Both hydrophilic and organically modified nanoclay were assessed in scope of this study. PVOH encourages the bonding of chitosan with hydrophilic but not hydrophobic nanoclay. Interestingly, both organic and hydrophilic nanoclay formed percolated network structures due to hydrogen bonding with chitosan. The clay limits phase separation between composite elements, and the network improved the strength, barrier, and antimicrobial properties. The properties of the nanocomposite prompts its application in food packaging. Network structures of clay were also formed by Cavallaro *et al.*[245] In this approach, pectin from apple and citrus and halloysite clay nanotubes were blended through solvent mixing. The pectin matrix forms strong hydrogen bonds with the nanoclays, which thoroughly disperse the particles at low loading. As the amount of clay in the system increases, network structures begin to percolate (Fig. 11). Interestingly, the mechanical properties of the composite are consistent, even at high nanoclay loading. However, the presence of network structures dramatically improves the thermal stability and elastic modulus. Flocculated silicate structures have also been reported in PLA *via* a melt extrusion method by Ray *et al.*[205] Hydroxyl terminated PLA is shown to enhance the anisotropy of the composite, with improved mechanical properties. This is largely a result of the hydroxyl functionality on PLA, which allows for edge–edge interactions amongst the randomly distributed silicate. This encourages flocculation, reinforcing the composite and reducing chain movement. The composite hence shows improvement in strength and modulus. Another study by Piekarska *et al.* also reports networks of clay in PLA (with the addition of cellulose fibers) for enhanced tensile strength and storage modulus.[206]

6.1.4.2 Films. Clay nanoparticle films have been demonstrated to further enhance the strength of the biobased composite. In fact, Nuzzo *et al.* report the formation of clay films in PLA matrices with polyamide.[207] The clay serves as a physical barrier at the polyamide/PLA interface, limiting polymer coalescence and allowing for co-continuous matrix formation, even at high PLA (70%) and low polyamide content (30%). The introduction of the polyamide/clay mixture to the PLA phase enhances the mechanical strength and thermal stability of the composite. The improvements in composite properties are hypothesized to be a result of slowed relaxation times. The ratio of filler to polymers is an essential consideration in maintaining optimal mechanical performance. Yao *et al.* formed films of clay in chitosan.[208] The strong ionic and hydrogen bonding between the clay and chitosan prompts the formation of sheets in the composite. The layered structure improves the mechanical strength and fire retardancy.

6.1.5 Iron oxide

6.1.5.1 Clusters and networks. Iron oxide can introduce exciting properties to biobased matrices, such as magnetism and thermal stability.[246] Magnetism in nanoparticle assemblies are more controllable than individual particles, with demonstrated improvement in magnetic response, multivalent interactions, and magnetic properties. Like other metals, the majority of work follows *in situ* methodologies, as size and assembly control are challenging. However, one work by Yang

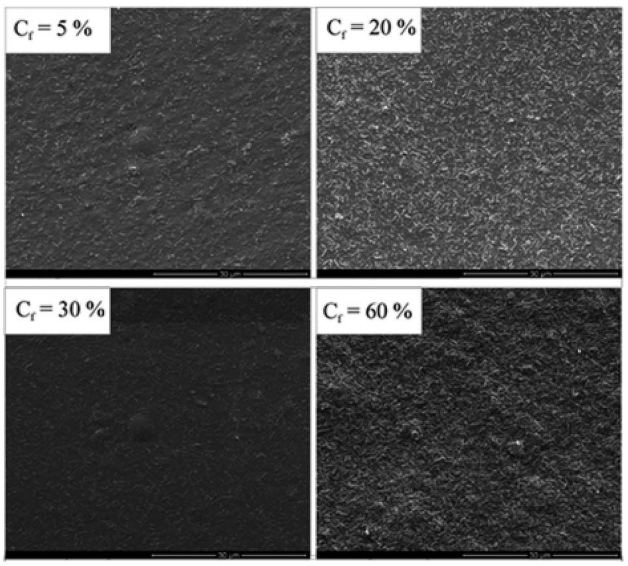

Fig. 11 Concentration driven clay networks in citrus pectin matrices for mechanical strength. This figure was adapted from ref. 244 with permission from the American Chemical Society, 2011.

et al. reported Fe_3O_4 cluster formation *via* blending in cellulose matrices.[199] Cluster size was stabilized in the matrix due to strong bonding with cellulose hydroxyl groups. The introduction of Fe_3O_4 clusters was shown to reduce the movement of cellulose chains in the composite, hindering crystallization processes and reducing tensile strength. In the same regard, elongation at break was increased. The composites also demonstrate sensing capacities against magnetic field and UV irradiation. Their high flexibility (without fracture) and thermal stability to 290 °C promotes their use as sensing devices.

6.2 Metallic nanoparticles

6.2.1 Gold and silver

6.2.1.1 Clusters and networks. Metallic nanoparticles such as gold and silver have been reported in biobased composite technologies. The number of studies in this area is considerable smaller than the quantity present in ceramic nanoparticles. This is largely due to the more severe aggregation in metallic nanoparticles because of the larger vdW attraction. However, with careful control of the assembly structure, diverse functionalities can still be introduced. Silver, for example can be used for antibacterial activity, and gold can offer unique surface plasmon resonance for sensor applications. Both silver and gold are electrical conductivity that can be used to fabricate electronics. Therefore, metallic nanoparticles have the potential to added great value to biobased polymers. In addition, assembling nanoparticles into well-defined structures can improve the properties provided by individual metallic nanoparticles.

Cheng *et al.* reported the formation of network structures of plasmonic gold nanorods in chiral nematic cellulose nanocrystals (with polyethylene glycol) for fluorescence.[186] It was discovered that the final properties of the composite are entirely dependent on the interactions between the nanocrystals and gold. When the gold was assigned a negative charge, strong electrostatic repulsion occurred with the cellulose nanocrystals. This allowed for the formation of a large helical pitch with a good chiral plasmonic patterns (Fig. 12). On the other hand, when the particles were positively charged, the nanocrystals formed a gel because of particle flocculation. Therefore the properties of the composite are driven by electrostatic interactions between the nanocrystals and nanorods, allowing for fluorescence and optical properties. Network structures of gold nanoparticles have also been demonstrated in chitosan matrices by Huang *et al.*[180] Again, charge was a determining factor in nanoparticle assembly. The nanoparticles were proven to assemble due to electrostatic interactions between citrate modified gold (negative) and chitosan (positive). With chitosan as the structural foundation material, the gold particles flocculated assembly patterns. As more layers of gold were added, the particles began to aggregate together to form a continuous, compact film. The multilayer system promotes high conductivity. Interestingly, the polymer–particle interactions are so strong that the coating can be exposed to extreme electrochemical conditions whilst maintaining its properties.

Hierarchical assembly structures of silver have demonstrated utility in biobased polymer matrices. Modification of the particle surface is responsible for the observed silver assembly, and polymers can be used to strategically determine the aggregation (or lack thereof). Trinh *et al.* used salinity to control the aggregation of silver nanoparticles.[194] With citrate surface modifications, salt was shown to aggregate the silver particles into network assemblies, an effect which is expedited with increasing salinity. Salinity induced aggregation slows in the

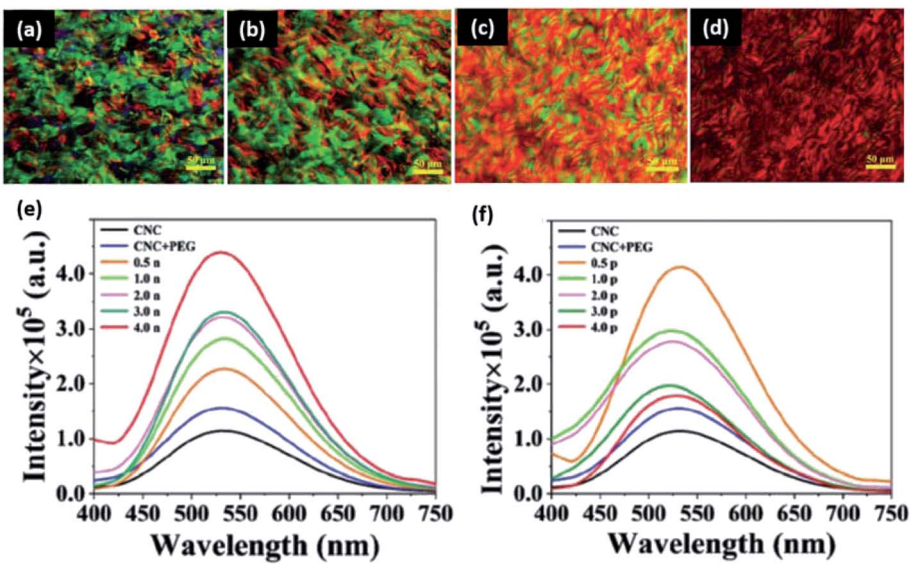

Fig. 12 Charge dependent gold nanorod networks in cellulose nanocrystal matrices for optoelectronic applications. Polarized optical microscopy images of (a) cellulose nanocrystals alone, (b) cellulose nanocrystals with PEG, (c) cellulose nanocrystals, PEG, and positive gold nanorods, and (d) cellulose nanocrystals, PEG, and negative gold nanorods. Fluorescence emission spectra (e) increases with negative nanorod loading, and (f) decreases with positive nanorod loading. Differences in the behavior of rods are a result of electrostatic interactions with the matrix material. This figure was adapted from ref. 185 with permission from Wiley, 2019.

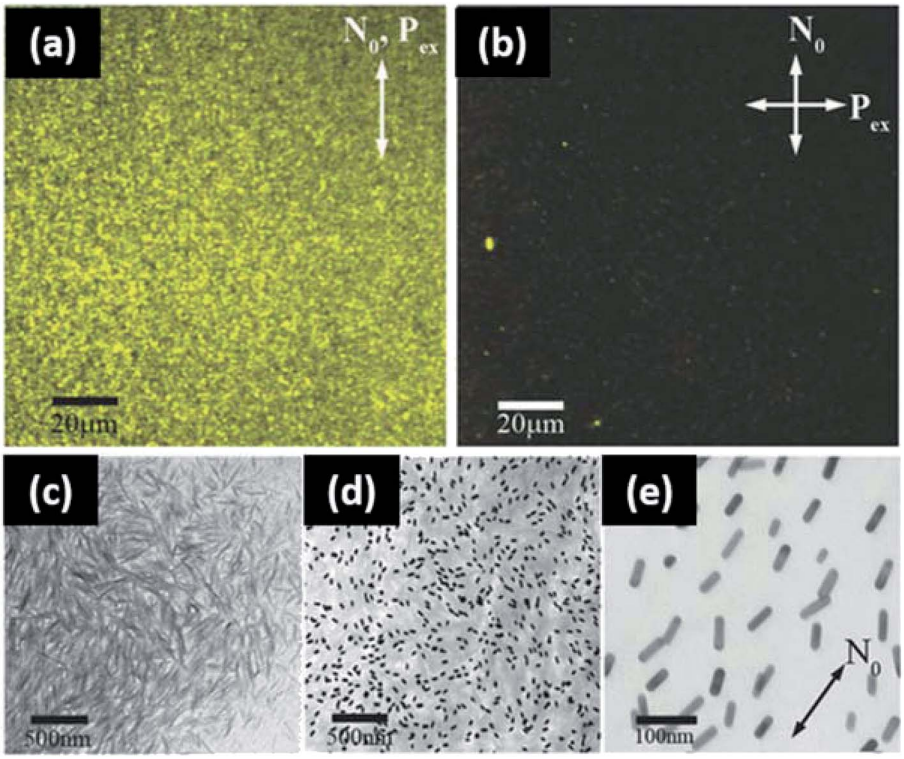

Fig. 13 Gold nanorod alignment in cellulose nanocrystal matrices for optoelectronic applications. Two-photon luminescence images of aligned gold nanorods in CNC with (a) the polarization excitation parallel to the aligned far field detector, (b) the polarization excitation perpendicular to the far field director, (c) TEM micrograph of CNCs alone, (d and e) TEM of aligned gold nanorods in CNCs. This figure was adapted from ref. 247, with permission from Wiley, 2014.

presence of hydroxyethyl cellulose (and stops completely in the case of its hydrophobic derivative). The authors propose that the aggregation differences are a result of the nanoparticle surface modification. For example, citrate may cover the surface and prevent the particles from aggregation, whereas salt induces aggregation. With the introduction of cellulose partially covering the silver surface, aggregation can occur at the expense of bridging. However, full surface coverage stabilizes the particles and inhibits aggregation. Network structures of silver nanoparticles have also been reported by Liu *et al.* in matrices including chiral nematic cellulose nanocrystals.[189] With alteration of the cellulose: silver ratio, the chiral reflectance was tuned and various iridescent colors were observed. The interaction between silver and cellulose was proven to be purely physical bonding, and silver did not disrupt the crystalline phases. The tunable optical properties of the material are proposed for specific wavelength absorption/identification applications, such as anti-counterfeit technology.

6.2.1.2 Films. Larger volumes of work in metallic nanoparticle self-assembly involve complex hierarchical structures and films. This is likely a result of concerns of reduced functionality (namely antibacterial efficacy and conductivity) in a poorly packed system. Films of gold nanoparticles have demonstrated utility in optical (polarizing) and conductive applications. For example, Liu *et al.* reported self-standing films of citrate modified gold nanoparticles in cellulose matrices for conductivity.[183] The incorporation of nanoparticles was not shown to impact the mechanical properties of the composite, and the tensile strength of cellulose was maintained. The mechanical strength of the material is hypothesized to be a result of strong interactions with the hydroxyl groups of the polymer matrix. Pinto *et al.* demonstrated that both vegetal and bacterial cellulose can also be used to assemble gold nanoparticles into films *via* layer-by-layer techniques.[247] However, in this study the cellulose behaves as a template for nanoparticle assembly into a film. It was proven that the type of cellulose fiber determines the final optical properties of the composite. Optical properties (and aggregation) can be further tuned by coating the gold with a shell of silica. Gold nanorod film alignments with cellulose nanocrystals (CNCs) were reported in a study by Liu *et al.*[248] Cellulose nanocrystal loading was found to drive isotropic or nematic alignments *via* the depletion interaction. The alignment of gold nanorods induces polarization effects in the film, and potential applications include smart windows and plasmonic polarizers (Fig. 13).

Films of silver nanoparticles have been reported more prevalently than gold nanoparticles, largely due to their antibacterial, additive manufacturing, and electronic utility. Dense film structures of silver optimize the inherent abilities of the nanoparticles, improving the functionality of the polymer matrix. For example, Martins *et al.* deposited silver films on cellulose fibers with different polyelectrolyte modifications (poly(diallyldimethylammonium chloride), poly(sodium 4-styrenesulfonate), poly(allylamine hydrochloride), and branched

polyethylenimine).[187] It was shown that the most homogenous deposition occurred with cationic and anionic polyelectrolytes. Cellulose–Ag nanocomposites were then integrated with starch matrices for antibacterial papers. The papers (with polyelectrolyte modification) were shown to be effective in *S. aureus* and *K. pneumoniae* bacterium at low nutrient concentrations. Cationic modifiers were most effective due to electrostatic interactions with anionic groups on the cell walls. Introduction of the nanofiller improved the mechanical and barrier properties of the starch papers. Elated, cellulose paper substrates were used to form films of silver nanowires *via* dip coating methods by Lee *et al.*[192] Silver nanowire interconnectivity is observed on the paper surface, though some have penetrated to the inner layers. Variation in silver density leads to anisotropic electrical conductivity. A single coating of silver was shown to improve the conductivity drastically. Increasing numbers of dip coatings provides further improvement. The cellulose paper structure, therefore, is a fitting template for the assembly of silver for improved material properties.

Other polymer matrices, such as wool, can be functionalized *via* the templated assembly of silver nanoparticles films (in tandem with silica nanoparticles).[191] In a study by Tang *et al.*, wool matrices were dipped in silica, and then silver (both at low pH). Layered nanoparticle assemblies were achieved as a result of strong hydrogen bonding. Interestingly, the wool fabrics can show bright colors due to silver plasmon resonance. The variation in color is mainly because of the geometry of the silver used in the coating, with green coming from nanoprisms and nanospheres, blue from nanoprisms alone, and red and yellow from nanodisks. Alongside the variation in color, the film promotes hydrophilicity and antibacterial efficacy. The properties of the film prompt its use in high wear textile applications.

7. Modelling and simulation on assembly of nanoparticles

Because the organization and distribution of nanoparticles play such important roles in determining the composite properties, it is critical to develop a comprehensive understanding of not only final structures but full dynamics of nanoparticle assembly in biobased polymer matrices. However, polymer nanocomposites feature complex physics at play on drastically different length and time scales, ranging from sub-nanoscale interactions between particles and polymers interactions (as discussed in previous sections) to clustering and percolation of nanoparticles into microstructures (as discussed in previous sections) to crack propagation and fracture on the macroscale. Computational modelling and simulations offer unparalleled abilities to analyze phenomena or processes of interest across the full spectrum of length and time scales. They are indispensable tools for establishing the processing-structure–property relationship for design of advanced polymer nanocomposites. Although many excellent reviews accounting for the theory and simulation of polymer nanocomposites already exist,[249–255] the majority discusses either petroleum based systems or generic model polymers. There are few computational studies dedicated to specific biobased nanocomposites. This section aims to outline the recent progress in understanding the assembly of nanoparticles in biobased polymer matrices through modelling and simulation.

Nanoparticle aggregation and assembly within nanocomposites has been modeled extensively on different scales using atomistic and coarse-grained molecular dynamics (MD), Monte Carlo (MC) methods, Brownian dynamics (BD), dissipative particle dynamics (DPD), self-consistent field theory (SCFT), density functional theory (DFT), and integral equation theories (also known as PRISM).[251,252,256] For example, Liu *et al.* utilized coarse-grained MD to study the dispersion and aggregation of nanocomposites.[257] Their work reveals the qualitative phase behavior of nanocomposites by changing both the polymer–particle interaction and nanoparticle concentration and identifies ideal conditions for creating homogeneous dispersions. Gervasio *et al.* developed a constant-number kinetic Monte Carlo (KMC) scheme to model the aggregation kinetics of ZnO nanoparticles and poly(methyl methacrylate) (PMMA) cosuspensions during drying (Fig. 14a).[258] The simulation successfully predicts average surface roughness of the dried nanocomposites that agrees well to the experimental value (Fig. 14b). To resolve the assembly structure and kinetics on the individual particle level, Lu *et al.* recently modeled the morphology of polymer nanocomposites comprised of

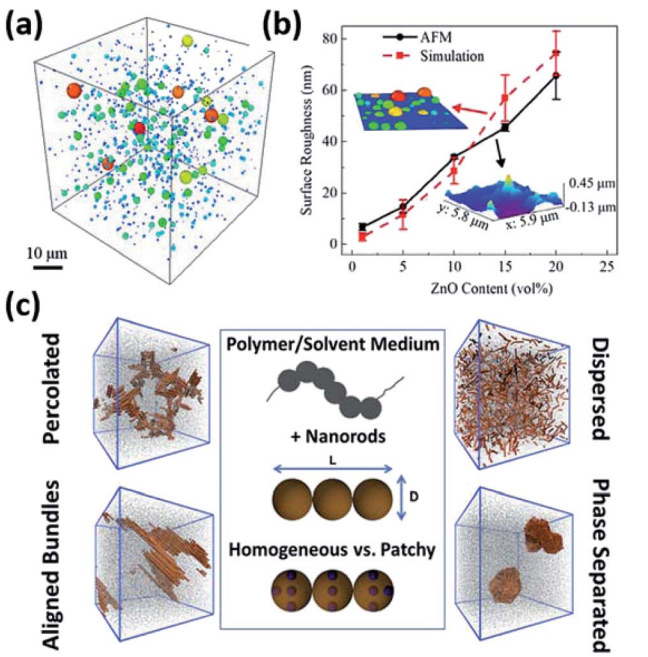

Fig. 14 (a) KMC simulation prediction of aggregation in 20 vol% ZnO–PMMA cosuspension and (b) comparison of the surface roughness of simulated dry sample to experimental results after 30 minutes of simulation time. The size of particle aggregates is also depicted by their colors, ranging from dark blue to dark red (50 nm to 15 μm respectively). Adapted from ref. 258 with permission from ACS Publications, 2019. (c) Coarse-grained MD simulations of different assembly structures of homogeneous and patchy nanorods in polymer nanocomposites. Adapted from ref. 259 with permission from the American Chemical Society, 2021.

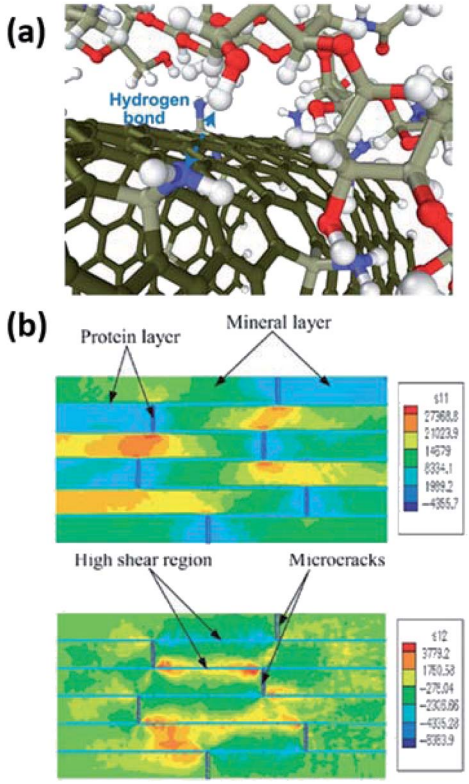

Fig. 15 (a) Atomistic MD simulation of hydrogen bond formation between functionalized carbon nanotubes and chitosan. Adapted from ref. 277 with permission from the American Chemical Society, 2016. (b) Simulation of cortical bone structure undergoing horizontal loading, showing colormaps of the normal stress in the loading direction (top) and shear stress along the mineral boundaries (bottom). Adapted from ref. 278 with permission from Elsevier, 2004.

nanorods, observing various modes of aggregation depending on the nanorod design as shown in Fig. 14c.[259]

Compared to petroleum-based synthetic polymers, computational modelling and simulation of the behavior of nanoparticles within biobased polymer matrices are far more challenging. This is largely attributed to less well-defined molecular architecture of natural polymers such as chitosan and starch as well as intricate interactions of polysaccharides with solvent molecules, ions, and nanoscale inclusions, which influence the arrangement and conformation of chains.[260–265] Significant progress has been made in the understanding of atomistic interactions and computation and prediction of mechanical properties of biobased nanocomposites with varying levels of hierarchy.[266–269] *Ab initio* simulation and classical MD provide great insight into nanoscale interactions among constituents of composites and elucidate the thermodynamic and dynamic behaviors at the filler–polymer interface from first principles with atomistic resolution (Fig. 15a).[262,270–277] Modelling efforts in mechanics of biobased nanocomposites exploit numerical approaches including MD, finite element method, and boundary element methods, as well as a variety of analytical methods and models to discover the structure–property relationship of these multicomponent systems, with prime examples being protein–mineral composites such as bone, shell, and wood (Fig. 15b).[268,278–282] A comprehensive account for these lines of research on biobased nanocomposites has been previously summarized.[266]

Despite extensive studies on these aspects of biobased nanocomposites, the assembly behavior of nanoparticles and underlying mechanisms remain surprisingly unexplored for biopolymer matrices. In an experimental study of ZnO assembly in modified starch (HES) and cellulose (HEC) composites, Olson *et al.* discovered that monomer conformations (α- and β-anomeric glycosides) have a significant impact on nanoparticle assembly.[165] Inspired by this work, Chen *et al.* applied the mesoscopic DPD method to investigate the effects of polymer chain conformation on nanoparticle assembly in biobased nanocomposite film formation.[93] The difference between HES and HEC polymers was modeled by modulating the rigidity of polymer chains. The results show that both very soft and very stiff polymers lead to clustered aggregates, while an intermediate stiffness results in dispersed aggregates. This behavior is reminiscent of the observation by Liu *et al.*,[257] although the mechanisms of the clustered–dispersed–clustered transition are completely different. Interestingly, the clustered aggregates favor distinct morphologies in soft and stiff matrices shown in Fig. 16a and b as a result of interplay between enthalpic and entropic effects in the polymer–particle–solvent three-phase system.[93] The assembly structures predicted by the DPD simulations match well with those in real HES and HEC nanocomposites. To bridge physical experiments and computer simulations, Olson *et al.* recently reported a BD-MC simulation of nanoparticle aggregation in biopolymer matrices using an interparticle potential derived from *in situ* AFM measurement of surface forces in the HES and HEC solutions.[239] The new AFM-derived potential agrees well with the theoretical interaction model between silica nanoparticles proposed by Snowden *et al.*,[283] considering the presence of various different absorbing and non-absorbing polymers, most notably HEC. The simulation incorporates rigid body motion of assembly with both translational and rotational diffusion, which has been shown to significantly influence the assembly structure of nanoparticles.[284,285] Similar to the scheme formulated by Gervasio *et al.*,[258] the reversible assembly of nanoparticles was modeled by MC steps with different Metropolis conditions for aggregation and separation of particles. The results demonstrate large-scale anisotropic cluster formation in the HEC nanocomposite and small dispersed cluster formation in the HES nanocomposite, which is highly consistent with fluorescent microscopy and confocal microscopy images of the physical systems (Fig. 16c–h). Despite the excellent agreement between the simulation and experimental results, it still lacks a clear understanding of underlying mechanisms that contribute to different nanoparticle interactions mediated by these biopolymers with complex molecular architecture. There exists a critical knowledge gap on micro-/mesostructure formation in biobased nanocomposites that links nanoparticle–biopolymer interactions at the atomic level to the macroscopic bulk properties. This structure–property relationship across several length scales challenges multiple fronts of computational modelling and simulations and warrants future studies.

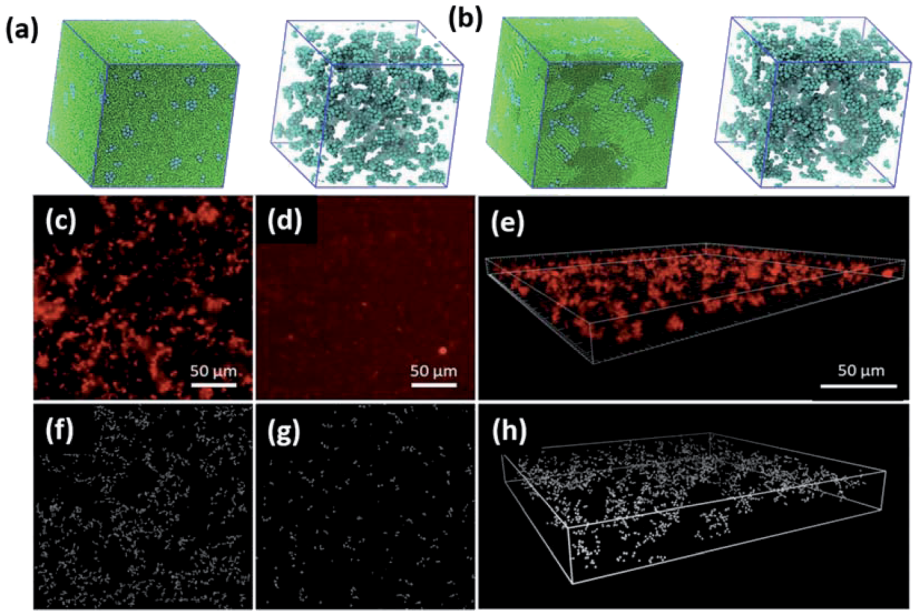

Fig. 16 (a and b) DPD simulations of dried polymer nanocomposites and internal particle assembly structures for (a) soft and (b) stiff polymer matrices. Adapted from ref. 93 with permission from the Royal Society of Chemistry, 2020. (c and d) Fluorescent microscopy images of silica nanoparticles in HEC and HES solutions, respectively. (e) Confocal 3D image of silica nanoparticle assembly in HEC solution. (f and g) BD simulation snapshots of nanoparticle assembly in HEC and HES, respectively. (h) Image of 3D view nanoparticle assembly in HEC in the simulation. Adapted from ref. 239 with permission from the Royal Society of Chemistry, 2021.

8. Conclusions

Biobased polymers are an attractive solution to address the petroleum plastic challenge, as they are derived from biomass and have reduced degradation times. However, the heterogeneous composition and inconsistent chemistry of biobased materials generate challenges in functionality and consistent performance. The incorporation of nanoparticles can introduce new properties and promote novel applications. Strategically assembling nanoparticles into hierarchical structures offers new opportunities to utilize these materials. It has been demonstrated that through careful experiment design, hierarchical assemblies including clusters and networks can be formed. To effectively formulate biobased nanocomposites for high value applications, interactions in biobased nanocomposites must be identified and optimized. Theoretical modelling and computational simulation are powerful tools in corroborating with experimental results and offering insight in fundamental interactions, which can further provide structure prediction and design. Work in this field is expected to grow as more experiments are carried out to probe the biobased polymer structures and interactions. We hope this review inspires more future work to explore nanoparticle self-assembly in biobased polymer matrices, expanding opportunities in applications of sustainable materials.

Author contributions

SJ and EO outline and wrote the majority of the review. FL assisted the review of *in situ* synthesis of nanocomposite. JB and XY wrote the review for the theory and simulation. YL assisted the graphic design. AT helped review the nanocomposite film for optical applications. RM helped review the nanocomposite in biobased foams. KV and GC helped the review in packaging applications. All authors contributed to discussion and revision of the manuscript.

Conflicts of interest

There are no conflicts to declare.

Acknowledgements

This project/material is based upon work supported by the Iowa Space Grant Consortium under NASA Award No. 80NSSC20M0107, Iowa EPSCoR Research Building Seed Grant, and EPSCoR Grant under NASA Award ID-NNH20ZHA001C. Acknowledgment is also made to the donors of the American Chemical Society Petroleum Research Fund for partial support of this research (Grant 60264-DNI7). S. J. and E. O. also thank the funding from the State of Iowa Biosciences Initiative. E. O. thanks the NASA fellowship from the Iowa Space Grant Consortium (ISGC) and Polymer and Food Protection Consortium for the support of her work. X. Y. and J. B. thank the Donors of the American Chemical Society Petroleum Research Fund for support. The review of simulation part was conducted under Grant No. 56884-DNI9. X. Y. thanks Dr Shensheng Chen for assisting in rendering polymer chain conformation in Fig. 1.

References

1 S. Farris, K. M. Schaich, L. S. Liu, L. Piergiovanni and K. L. Yam, Development of polyion-complex hydrogels as

an alternative approach for the production of biobased polymers for food packaging applications: a review, *Trends Food Sci. Technol.*, 2009, **20**, 316–332.

2 V. Siracusa, P. Rocculi, S. Romani and M. D. Rosa, Biodegradable polymers for food packaging: a review, *Trends Food Sci. Technol.*, 2008, **19**, 634–643.

3 S. C. Rasmussen, From Parkesine to Celluloid: The Birth of Organic Plastics, *Angew. Chem., Int. Ed.*, 2021, **60**, 8012–8016.

4 R. Batchelor, *Henry Ford Mass Production, Modernism and Design*, New York City, New York, Manchester, United Kingdom, 1994.

5 Q. R. Skrabec, *The Green Vision of Henry Ford and George Washington Carver*, McFarland &. Company, Inc., Jefferson, North Carolina, 2013.

6 A. Chamas, H. Moon, J. Zheng, Y. Qiu, T. Tabassum, J. H. Jang, M. Abu-Omar, S. L. Scott and S. Suh, Degradation Rates of Plastics in the Environment, *ACS Sustainable Chem. Eng.*, 2020, **8**, 3494–3511.

7 S. Peressini, B. Bravin, R. Lapasin, C. Rizzotti and A. Sensidoni, Starch-methylcellulose based edible films: rheological properties of film-forming dispersions, *J. Food Eng.*, 2003, **59**, 25–32.

8 M. Petersson and M. Stading, Water vapour permeability and mechanical properties of mixed starch–monoglyceride films and effect of film forming conditions, *Food Hydrocolloids*, 2005, **19**, 123–132.

9 A. K. Mohanty, S. Vivekanandhan, J.-M. Pin and M. Mirsa, Composites from renewable and sustainable resources: Challenges and innovations, *Science*, 2018, **362**, 536–542.

10 N. Singh, J. Singh, L. Kaur, N. S. Sodhi and B. S. Gill, Morphological, thermal and rheological properties of starches from different botanical sources, *Food Chem.*, 2003, **81**, 219–231.

11 D. Lavanya, P. Kulkarni, M. Dixit, P. K. Raavi and L. N. V. Krishna, Sources of cellulose and their applications – a review, *International Journal of Drug Formulation and Research*, 2011, **2**, 19–38.

12 S. RameshKumar, P. Shaiju, K. E. O'Connor and P. R. Babu, Bio-based and biodegradable polymers – state-of-the-art, challenges and emerging trends, *Curr. Opin. Green Sustain. Chem.*, 2020, **21**, 75–81.

13 A. Munoz-Bonilla, C. Echeverria, A. Sonseca, M. P. Arrieta and M. Fernandez-Garcia, Bio-Based Polymers with Antimicrobial Properties towards Sustainable Development, *Materials*, 2019, **12**, 641.

14 B. Hu, S. B. Wang, K. Wang, M. Zhang and S. H. Yu, Microwave-Assisted Rapid Facile "Green" Synthesis of Uniform SIiver Nanoparticles: Self-Assembly into Multilayer Films and Their Optical Properties, *J. Phys. Chem. C*, 2008, **112**, 11169–11174.

15 D. Mahanta, U. Manna, G. Madras and S. Patil, Multilayer Self-Assembly of TiO_2 Nanoparticles and Polyaniline-Grafted-Chitosan Copolymer (CPANI) for Photocatalysis, *ACS Appl. Mater. Interfaces*, 2011, **3**, 84–92.

16 A. Sorrentino, G. Gorrasi and V. Vittoria, Potential Perspectives of Bio-Nanocomposites for Food Packaging Applications, *Trends Food Sci. Technol.*, 2007, **18**, 84–95.

17 M. L. Lopez-Quintanilla, S. Sánchez-Valdés, L. F. R. d. Valle and F. J. Medellín-Rodríguez, Effect of some compatibilizing agents on clay dispersion of polypropylene–clay nanocomposites, *J. Appl. Polym. Sci.*, 2006, **100**, 4748–4756.

18 W. Lertwimmolnun and B. Vergnes, Influence of compatibilizer and processing conditions on the dispersion of nanoclay in a polypropylene matrix, *Polymer*, 2005, **46**, 3462–3471.

19 A. B. Morgan and J. D. Harris, Effects of organoclay Soxhlet extraction on mechanical properties, flammability properties and organoclay dispersion of polypropylene nanocomposites, *Polymer*, 2003, **44**, 2313–2320.

20 M. Kato, M. Matsushita and K. Fukumori, Development of a new production method for a polypropylene–clay nanocomposite, *Polym. Eng. Sci.*, 2004, **44**, 1205–1211.

21 P. Zhang and T. Kraus, Anisotropic nanoparticles as templates for the crystalline structure of an injection-molded isotactic polypropylene/TiO_2 nanocomposite, *Polymer*, 2017, **130**, 161–169.

22 P. A. Zapata, A. Zenteno, N. Amigo, F. M. Rabagliati, F. Sepulveda, F. Catalina and T. Corrales, Study on the photodegradation of nanocomposites based on polypropylene and TiO_2 nanotubes, *Polym. Degrad. Stab.*, 2016, **133**, 101–107.

23 D. Aydemir, G. Uzun, H. Gumus, S. Yidiz, S. Gumus, T. Bardak and G. Gunduz, Nanocomposites of polypropylene/nano titanium dioxide: effect of loading rates of nano titanium dioxide, *Mater. Sci.*, 2016, **22**, 364–369.

24 J. Hu, L. Zhang, Z. M. Dang and D. Wang, Improved dielectric properties of polypropylene-based nanocomposites via co-filling with zinc oxide and barium titanate, *Compos. Sci. Technol.*, 2017, **148**, 20–26.

25 K. A. Bustos-Torres, S. Vazquez-Rodriguez, A. M.-d. l. Cruz, S. Sepulveda-Guzman, R. Benavides, R. Lopez-Gonzalez and L. M. Torres-Martínez, Influence of the morphology of ZnO nanomaterials on photooxidation of polypropylene/ZnO composites, *Mater. Sci. Semicond. Process.*, 2017, **68**, 217–225.

26 W. Yuan, F. Wang, Z. Chen, C. Gao, P. Liu, Y. Ding, S. Zhang and M. Yang, Efficient grafting of polypropylene onto silica nanoparticles and the properties of PP/PP-*g*-SiO_2 nanocomposites, *Polymer*, 2018, **151**, 242–249.

27 G. Cao, H. Lin, P. Kannan, C. Wang, Y. Zhong, Y. Huang and Z. Guo, Enhanced antibacterial and food simulant activities of silver nanoparticles/polypropylene nanocomposite films, *Langmuir*, 2018, **34**, 14537–14545.

28 A. P. Bafana, X. Yan, X. Wei, M. Patel, Z. Guo, S. Wei and E. K. Wujcik, Polypropylene nanocomposites reinforced with low weight percent graphene nanoplatelets, *Composites, Part B*, 2017, **109**, 101–107.

29 S. Fazil, S. Saeed, M. Waseem, W. Rehman, M. Bangesh and K. Liaqat, Improving the mechanical and thermal

properties of chemically modified graphene oxide/polypropylene nanocomposite, *Polym. Compos.*, 2017, **39**, 1635–1642.

30 G. V. Nguyen, H. Thai, D. H. Mai, T. T. Huu, T. D. Lam and T. M. Vu, Effect of titanium dioxide on the properties of polyethylene/TiO_2 nanocomposites, *Composites, Part B*, 2013, **45**, 1192–1198.

31 M. Romero-Saez, L. Y. Jaramillo, R. Saravanan, N. Benito, E. Pabon, E. E. M. Vargas and F. Garcia, Notable photocatalytic activity of TiO_2–polyethylene nanocomposites for visible light degradation of organic pollutants, *eXPRESS Polym. Lett.*, 2017, **11**, 899–909.

32 Z. N. Hashemabad, B. Shabanpour, H. Azizi, S. M. Ojagh and A. Alishahi, Effect of TiO_2 Nanoparticles on the Antibacterial and Physical Properties of Low-Density Polyethylene Film, *Polym.-Plast. Technol. Eng.*, 2017, **56**, 1516–1527.

33 M. Catauro, C. Scolaro and A. Visco, Mechanical Performance of Polyethylene Joints Based on Nanocomposites Doped with Titanium Dioxide, *Macromol. Symp.*, 2020, **389**, 190085–190088.

34 L. Zhang, M. M. Khani, T. M. Krentz, Y. Huang, Y. Zhou, B. C. Benicewicz, J. K. Nelson and L. S. Shadler, Suppression of space charge in crosslinked polyethylene filled with poly(stearyl methacrylate)-grafted SiO_2 nanoparticles, *Appl. Phys. Lett.*, 2017, **110**, 123903.

35 A. Akbari, R. Tegani and B. Pourabbas, Synthesis of high dispersible hydrophilic poly(ethylene glycol)/vinyl silane grafted silica nanoparticles to fabricate protein repellent polyethylene nanocomposite, *Eur. Polym. J.*, 2016, **81**, 86–97.

36 J. Ahmed, Y. A. Arfat, H. Al-Attar, R. Auras and M. Ejaz, Rheological, structural, ultraviolet protection and oxygen barrier properties of linear low-density polyethylene films reinforced with zinc oxide (ZnO) nanoparticles, *Food Packag. Shelf Life*, 2017, **13**, 20–26.

37 E. Helal, C. Pottier, E. David, M. Frechette and N. R. Demarquette, Polyethylene/thermoplastic elastomer/zinc oxide nanocomposites for high voltage insulation applications: dielectric, mechanical and rheological behavior, *Eur. Polym. J.*, 2018, **100**, 258–269.

38 E. Helal, N. R. Demarquette, E. David and M. F. Frechette, Evaluation of dielectric behavior of polyethylene/thermoplastic elastomer blends containing zinc oxide (ZnO) nanoparticles for high voltage insulation, in *IEEE Electrical Insulation Conference*, Montreal, QC, Canada, 2016.

39 A. M. Pourrahimi, T. A. Hoang, D. Liu, L. K. H. Pallon, S. Gubanski, R. T. Olsson, U. W. Gedde and M. S. Hedenqvist, Highly efficient interfaces in nanocomposites based on polyethylene and ZnO nano/hierarchical particles: a novel approach toward ultralow electrical conductivity, *Adv. Mater.*, 2016, **28**, 8651–8657.

40 S. Siddque, G. D. Smith, K. Yates, A. K. Mishra, K. Matthews, L. J. Csetenyi and J. Njiguna, Structural and thermal degradation behaviour of reclaimed clay nano-reinforced low-density polyethylene nanocomposites, *J. Polym. Res.*, 2019, **26**, 154–168.

41 W. L. Oliani, D. Parra, N. Lincopan and V. Rangari, Preparation and characterization of polyethylene nanocomposites with clay and silver nanoparticles, in *Characterization of Minerals, Metals, and Materials 2017*, ed. S. Ikhmayies, B. Li, J. S. Carpenter, J. Li, J. Y. Hwang, S. N. Monteiro, D. Firrao, M. Zhang, Z. Peng, J. P. Escobedo-Diaz, C. Bai, Y. E. Kalay, R. Goswami and J. Kim, Springer Nature, Cham, Switzerland, 2017.

42 D. Patra, P. Vangal, A. A. Cain, C. Cho, O. Regev and J. C. Grunlan, Inorganic Nanoparticle Thin Film that Suppresses Flammability of Polyurethane with only a Single Electrostatically-Assembled Bilayer, *ACS Appl. Mater. Interfaces*, 2014, **6**, 16903–16908.

43 Y. Shi, C. Liu, L. Fu, F. Yang, Y. Lv and B. Yu, Hierarchical assembly of polystyrene/graphitic carbon nitride/reduced graphene oxide nanocomposites toward high fire safety, *Composites, Part B*, 2019, **179**, 107541–107549.

44 Y. C. Li, J. Schulz, S. Mannen, C. Delhom, B. Condon, S. Chang, M. Zammarano and J. C. Grunlan, Flame Retardant Behavior of Polyelectrolyte–Clay Thin Film Assemblies on Cotton Fabric, *ACS Nano*, 2010, **4**, 3325–3337.

45 F. B. Dhieb, E. J. Dil, S. H. Tabatabaei, F. Mighri and A. Ajji, Effect of nanoclay orientation on oxygen barrier properties of LbL nanocomposite coated films, *RSC Adv.*, 2019, **9**, 1632–1641.

46 C. Peng, Y. S. Thio and R. A. Gerhardt, Enhancing the Layer-by-Layer Assembly of Indium Tin Oxide Thin Films by Using Polyethyleneimine, *J. Phys. Chem. C*, 2010, **114**, 9685–9692.

47 M. T. Masood, J. A. Heredia-Guerrero, L. Cesracciu, F. Palazon, A. Athanassiou and I. S. Bayer, Superhydrophobic high impact polystyrene (HIPS) nanocomposites with wear abrasion resistance, *Chem. Eng. J.*, 2017, **322**, 10–21.

48 M. N. Tchoul, S. P. Fillery, H. Koerner, L. F. Drummy, F. T. Oyerokun, P. A. Mirau, M. F. Durstock and R. A. Vaia, Assemblies of Titanium Dioxide–Polystyrene Hybrid Nanoparticles for Dielectric Applications, *Chem. Mater.*, 2010, **22**, 1749–1759.

49 R. Nutenki, P. R. Darapureddi, R. R. Nayak and S. I. Kattimuttathu, Amphiphilic comb-like polymer-modified graphene oxide and its nanocomposite with polystyrene via emulsion polymerization, *Colloid Polym. Sci.*, 2018, **296**, 133–144.

50 P. Krystosiak, W. Tomaszewski and E. Megiel, High-density polystyrene-grafted silver nanoparticles and their use in the preparation of nanocomposites with antibacterial properties, *J. Colloid Interface Sci.*, 2017, **498**, 9–21.

51 X. Hu, N. Ren, Y. Chao, H. Lan, X. Yan, Y. Sha, X. Sha and Y. Bai, Highly aligned graphene oxide/poly(vinyl alcohol) nanocomposite fibers with high-strength, antiultraviolet and antibacterial properties, *Composites, Part A*, 2017, **102**, 297–304.

52 B. Li and E. Manias, Increased dielectric breakdown strength of polyolefin nanocomposites via nanofiller alignment, *MRS Adv.*, 2016, **2**, 1–6.
53 L. Gan, F. Qiu, Y. B. Hao, K. Zhang, Z. Y. Zhou, J. B. Zeng and M. Wang, Shear-induced orientation of functional graphene oxide sheets in isotactic polypropylene, *J. Mater. Sci.*, 2016, **51**, 5185–5195.
54 M. Mashkour, T. Kimura, F. Kimura, M. Mashkour and M. Tajvidi, Tunable Self-Assembly of Cellulose Nanowhiskers and Polyvinyl Alcohol Chains Induced by Surface Tension Torque, *Biomacromolecules*, 2014, **15**, 60–65.
55 W. Chen and X. Tao, Self-Organizing Alignment of Carbon Nanotubes in Thermoplastic Polyurethane, *Macromol. Rapid Commun.*, 2005, **26**, 1763–1767.
56 M. Okamoto, P. H. Nam, P. Maiti, T. Kotaka, N. Hasegawa and A. Usuki, A House of Cards Structure in Polypropylene/Clay Nanocomposites under Elongational Flow, *Nano Lett.*, 2001, **1**, 295–298.
57 B. Li, P. I. Xidas, K. S. Triantafyllidis and E. Manias, Effect of crystal orientation and nanofiller alignment on dielectric breakdown of polyethylene/montmorillonite nanocomposites, *Appl. Phys. Lett.*, 2017, **111**, 82906–82910.
58 R. Haggenmueller, C. Guthy, J. R. Lukes and J. E. Fischer, Single Wall Carbon Nanotube/Polyethylene Nanocomposites: Thermal and Electrical Conductivity, *Macromolecules*, 2007, **40**, 2417–2421.
59 A. J. Waddon, L. Zheng, R. J. Farris and E. B. Coughlin, Nanostructured Polyethylene–POSS Copolymers: Control of Crystallization and Aggregation, *Nano Lett.*, 2002, **2**, 1149–1155.
60 R. W. Zehner, W. A. Lopes, T. L. Morkved, H. Jaeger and L. R. Sita, Selective Decoration of a Phase-Separated Diblock Copolymer with Thiol-Passivated Gold Nanocrystals, *Langmuir*, 1998, **14**, 241–244.
61 M. R. Bockstaller, Y. Lapetnikov, S. Margel and E. L. Thomas, Size-Selective Organization of Enthalpic Compatibilized Nanocrystals in Ternary Block Copolymer/Particle Mixtures, *J. Am. Chem. Soc.*, 2003, **125**, 5276–5277.
62 A. Kausar, Investigation on Self-assembled Blend Membranes of Polyethylene-*block*-poly(ethylene glycol)-*block*-polycaprolactone and Poly(styrene-*block*-methyl methacrylate) with Polymer/Gold Nanocomposite Particles, *Polym.-Plast. Technol. Eng.*, 2015, **54**, 1794–1802.
63 J. Su, L. Zhu, P. Geng and G. Chen, Self-assembly graphitic carbon nitride quantum dots anchored on TiO_2 nanotube arrays: an efficient heterojunction for pollutants degradation under solar light, *J. Hazard. Mater.*, 2016, **316**, 159–168.
64 N. Suzuki, M. Imura, Y. Nemoto, X. Jiang and Y. Yamauchi, Mesoporous SiO_2 and Nb_2O_5 thin films with large spherical mesopores through self-assembly of diblock copolymers: unusual conversion to cuboidal mesopores by Nb_2O_5 crystal growth, *CrystEngComm*, 2011, **13**, 40–43.
65 V. G. Kotlyar, D. A. Olyanich, T. V. Utas, A. V. Zotov and A. A. Saranin, Self-assembly of C_{60} fullerenes on quasi-one-dimensional Si(111)4 × 1-In surface, *Surf. Sci.*, 2012, **606**, 23–24.
66 G. Tong, J. Guan and Q. Zhang, In Situ Generated Gas Bubble-Directed Self-Assembly: Synthesis, and Peculiar Magnetic and Electrochemical Properties of Vertically Aligned Arrays of High-Density Co_3O_4 Nanotubes, *Adv. Funct. Mater.*, 2012, **23**, 2406–2414.
67 B. Ghanbarzadeh, S. A. Oleyaei and H. Almasi, Nanostructured Materials Utilized in Biopolymer-based Plastics for Food Packaging Applications, *Crit. Rev. Food Sci. Nutr.*, 2015, **55**, 1699–1723.
68 F. W. Xie, E. Pollet, P. J. Halley and L. Averous, Starch-based nano-biocomposites, *Prog. Polym. Sci.*, 2013, **38**, 1590–1628.
69 M. M. Reddy, S. Vivekanandhan, M. Misra, S. K. Bhatia and A. K. Mohanty, Biobased plastics and bionanocomposites: current status and future opportunities, *Prog. Polym. Sci.*, 2013, **38**, 1653–1689.
70 Z. Xue, C. Yan and T. Wang, From atoms to lives: the evolution of nanoparticle assemblies, *Adv. Funct. Mater.*, 2019, **29**, 1807658.
71 M. A. Boles, M. Engel and D. V. Talapin, Self-Assembly of Colloidal Nanocrystals: From Intricate Structures to Functional Materials, *Chem. Rev.*, 2016, **116**(18), 11220–11289.
72 Y. J. Min, M. Akbulut, K. Kristiansen, Y. Golan and J. Israelachvili, The role of interparticle and external forces in nanoparticle assembly, *Nat. Mater.*, 2008, **7**(7), 527–538.
73 M. A. Boles, D. Ling, T. Hyeon and D. V. Talapin, The surface science of nanocrystals, *Nat. Mater.*, 2016, **15**(2), 141–153.
74 S. K. Kumar and R. Krishnamoorti, Nanocomposites: Structure, Phase Behavior, and Properties, *Annu. Rev. Chem. Biomol. Eng.*, 2010, **1**, 37–58.
75 J. Jancar, J. F. Douglas, F. W. Starr, S. K. Kumar, P. Cassagnau, A. J. Lesser, S. S. Sternstein and M. J. Buehler, Current issues in research on structure–property relationships in polymer nanocomposites, *Polymer*, 2010, **51**, 3321–3343.
76 M. E. Mackay, A. Tuteja, P. M. Duxbury, C. J. Hawker, B. V. Horn, Z. Guan, G. Chen and R. S. Krishnan, General Strategies for Nanoparticle Dispersion, *Science*, 2006, **311**, 1740–1743.
77 S. Jiang, A. Van Dyk, A. Maurice, J. Bohling, D. Fasano and S. Brownell, Design colloidal particle morphology and self-assembly for coating applications, *Chem. Soc. Rev.*, 2017, **46**(12), 3792–3807.
78 N. A. Kotov, F. C. Meldrum, C. Wu and J. H. Fendler, Monoparticulate layer and Langmuir–Blodgett-type multiparticulate layers of size-quantized cadmium sulfide clusters: a colloid-chemical approach to superlattice construction, *J. Phys. Chem.*, 1994, **98**, 2735–2738.
79 A. Taleb, C. Petit and M. Pileni, Synthesis of highly monodisperse silver nanoparticles from AOT reverse micelles: a way to 2D and 3D self-organization, *Chem. Mater.*, 1997, **9**, 950–959.

80 F. Liu, E. Mascheroni and L. Piergiovanni, The Potential of NanoCellulose in the Packaging Field: A Review, *Packag. Technol. Sci.*, 2015, **28**, 475–508.
81 Y. Habibi, L. A. Lucia and O. J. Rojas, Cellulose Nanocrystals: Chemistry, Self-Assembly, and Applications, *Chem. Rev.*, 2010, **110**, 3479–3500.
82 R. Shenhar, T. B. Norsten and V. M. Rotello, Polymer-Mediated Nanoparticle Assembly: Structural Control and Applications, *Adv. Mater.*, 2005, **17**, 657–669.
83 K. Thorkelsson, P. Bai and T. Xu, Self-assembly and applications of anisotropic nanomaterials: a review, *Nano Today*, 2015, **10**, 48–66.
84 J. Isrealachvili, *Intermolecular and Surface Forces*, 3edn, Academic Press, Cambridge, MA, 2015, p. 1084.
85 H. Kim, S. Kobayashi, M. A. AbdurTahim, M. J. Zhang, A. Khusainova, M. A. Hillmyer, A. A. Abdala and C. W. Macosko, Graphene/polyethylene nanocomposites: effect of polyethylene functionalization and blending methods, *Polymer*, 2011, **52**, 1837–1846.
86 M. Tanahashi, Development of Fabrication Methods of Filler/Polymer Nanocomposites: With Focus on Simple Melt-Compounding-Based Approach without Surface Modification of Nanofillers, *Materials*, 2010, **3**, 1593–1619.
87 P. Tiemblo, E. Benito, N. Garcia, A. Esteban-Cubillo, R. Pina-Zapardiel and C. Pecharroman, Multiscale gold and silver plasmonic plastics by melt compounding, *RSC Adv.*, 2012, **2**, 915–919.
88 C. Radheshkumar and H. Munstedt, Morphology and mechanical properties of antimicrobial polyamide/silver composites, *Mater. Lett.*, 2005, **59**, 1949–1953.
89 W. Chen, S. Li, C. Chen and L. Yan, Self-Assembly and Embedding of Nanoparticles by In Situ Reduced Graphene for Preparation of a 3D Graphene/Nanoparticle Aerogel, *Adv. Mater.*, 2011, **23**, 5679–5683.
90 M. Kaushika and A. Moores, Review: nanocelluloses as versatile supports for metal nanoparticles and their applications in catalysis, *Green Chem.*, 2016, **18**, 622–637.
91 C. Zhu, S. Monti and A. P. Mathew, Cellulose Nanofiber–Graphene Oxide Biohybrids: Disclosing the Self-Assembly and Copper-Ion Adsorption Using Advanced Microscopy and ReaxFF Simulations, *ACS Nano*, 2018, **12**, 7028–7038.
92 J. Majoinen, J. Hassinen, J. S. Haataja, H. T. Rekola, E. Kontturi, M. A. Kostianinen, R. H. A. Ras, P. Torma and O. Ikkala, Chiral Plasmonics Using Twisting along Cellulose Nanocrystals as a Template for Gold Nanoparticles, *Adv. Mater.*, 2016, **28**, 5262–5267.
93 S. Chen, E. Olson, S. Jiang and X. Yong, Nanoparticle assembly modulated by polymer chain conformation in composite materials, *Nanoscale*, 2020, **12**, 14560–14572.
94 N. Singh, Extrusion Problems Solved: Food, Pet Food and Feed By M. N. Riaz and G. J. Rokey Cambridge: Woodhead Publishing. Pp. 154. ISBN: 978-1-85573-558-3. Price: US $210, *Int. J. Food Sci. Technol.*, 2014, **49**(2), 655.
95 H. J. Chung, Q. Liu, E. Donner and R. Hoover, Composition, molecular structure, properties, and in vitro digestibility of starches from newly released Canadian pulse cultivars, *Cereal Chem.*, 2008, **85**, 471–479.
96 R. Hoover and W. S. Ratnayake, Starch Characteristics of black bean, chick pea, lentil, navy bean. and pinto beancultivars grown in Canada, *Food Chem.*, 2002, **78**, 489–498.
97 S. Hizukuri, Relationship between the distribution of the chain length of amylopectin and the crystalline structure of starch granules, *Carbohydr. Res.*, 1985, **141**, 295–306.
98 S. Kobayashi, S. J. Schwartz and D. R. Lineback, Comparison of the structure of amylopectins from different wheat varieties, *Cereal Chem.*, 1986, **68**, 71–74.
99 Y. Takeda, S. Hizukuri, C. Takeda and A. Suzuki, Structures of branched molecules of amyloses of various origins and the molar fractions of branched and unbranched molecules, *Carbohydr. Res.*, 1987, **165**, 139–145.
100 M. J. Gidley and S. M. Bociek, Carbon-13 CP/MAS NMR studies of amylose inclusion complexes, cyclodextrins, and the amorphous phase of starch granules: relationships between glycosidic linkage conformation and solid-state carbon-13 chemical shifts, *J. Am. Chem. Soc.*, 1988, **110**, 3820–3829.
101 R. Hoover, Composition, molecular structure, and physicochemical properties of tuber and root starches: a review, *Carbohydr. Polym.*, 2001, **45**, 253–267.
102 A. C. O'Sullivan, Cellulose: the structure slowly unravels, *Cellulose*, 1996, **4**, 173–207.
103 T. Shen, P. Langan, A. D. French, G. P. Johnson and S. Gnanakaran, Conformational Flexibility of Soluble Cellulose Oligomers: Chain Length and Temperature Dependence, *J. Am. Chem. Soc.*, 2009, **2009**, 14786–14794.
104 I. K. Park, H. Sun, S. H. Kim, Y. Kim, G. E. Kim, Y. Lee, H. R. Choi, J. Suhr and J. D. Nam, Solvent-free bulk polymerization of lignin–polycaprolactone (PCL) copolymer and its thermoplastic characteristics, *Sci. Rep.*, 2019, **9**, 1–11.
105 S. Skovstrup, S. G. Hansen, T. Skrydstrup and B. Schiøtt, Conformational Flexibility of Chitosan: A Molecular Modeling Study, *Biomacromolecules*, 2010, **11**, 3196–3207.
106 K. V. Apryatina, E. K. Tkachuk and L. A. Smirnova, Influence of macromolecules conformation of chitosan on its graft polymerization with vinyl monomers and the copolymer properties, *Carbohydr. Polym.*, 2020, **235**, 115954–115963.
107 S. Iannace, L. Sorrentino and E. D. Maio, Biodegradable biomedical foam scaffolds, in *Biomedical Foams for Tissue Engineering Applications*, ed. P. A. Netti, Woodhead Publishing, Cambridge, United Kingdom, 2014, pp. 163–187.
108 A. Milionis, R. Ruffilli and I. S. Bayer, Superhydrophobic nanocomposites from biodegradable thermoplastic starch composites (Mater-Bi®), hydrophobic nano-silica and lycopodium spores, *RSC Adv.*, 2014, **4**, 34395–34404.
109 S. Zheng, D. A. Bellido-Aguilar, Y. Huang, X. Zeng, Q. Zhang and Z. Chen, Mechanically robust hydrophobic bio-based epoxy coatings for anti-corrosion application, *Surf. Coat. Technol.*, 2019, **363**, 43–50.

110 S. Ni, H. Zhang, P. M. Godwin, H. Dai and H. Xiao, ZnO nanoparticles enhanced hydrophobicity for starch film and paper, *Mater. Lett.*, 2018, **230**, 207–210.

111 M. P. Indumathi, K. S. Sarojini and G. R. Rajarajeswari, Antimicrobial and biodegradable chitosan/cellulose acetate phthalate/ZnO nano composite films with optimal oxygen permeability and hydrophobicity for extending the shelf life of black grape fruits, *Int. J. Biol. Macromol.*, 2019, **132**, 1112–1120.

112 X. Wang, S. Liu, H. Chang and J. Liu, Sol–Gel Deposition of TiO_2 Nanocoatings on Wood Surfaces with Enhanced Hydrophobicity and Photostability, *Wood Fiber Sci.*, 2014, **46**, 109–117.

113 V. Goudarzi, I. Shahabi-Ghahfarrokhi and A. Babaei-Ghazvini, Preparation of Ecofriendly, UV-protective food packaging material by starch/TiO_2 bio-nanocomposite: characterization, *Int. J. Biol. Macromol.*, 2017, **95**, 306–313.

114 P. Kampeerapappun, D. Aht-ong, D. Pentrakoon and K. Srikulkit, Preparation of cassava starch/montmorillonite composite film, *Carbohydr. Polym.*, 2013, **67**, 155–163.

115 X. Wang, P. Qu and L. Zhang, Thermal and structure properties of biobased cellulose nanowhiskers/poly(lactic acid) nanocomposites, *Fibers Polym.*, 2014, **15**, 302–306.

116 A. Khan, R. A. Khan, S. Salmieri, C. L. Tien, B. Riedl, J. Bouchard, G. Chauve, V. Tan, M. R. Kamal and M. Lacroix, Mechanical and barrier properties of nanocrystalline cellulose reinforced chitosan based nanocomposite films, *Carbohydr. Polym.*, 2012, **90**, 1601–1608.

117 S. M. Noorbakhsh-Soltani, M. M. Zerafat and S. Sabbaghi, A comparative study of gelatin and starch-based nano-composite films modified by nano-cellulose and chitosan for food packaging applications, *Carbohydr. Polym.*, 2018, **189**, 48–55.

118 Y. Habibi, L. A. Lucia and O. J. Rojas, Cellulose Nanocrystals: Chemistry, Self-Assembly, and Applications, *Chem. Rev.*, 2010, **110**(6), 3479–3500.

119 K. Shahzadi, L. Wu, X. Ge, F. Zhao, H. Li, S. Pang, Y. Jiang, J. Guan and X. Mu, Preparation and characterization of bio-based hybrid film containing chitosan and silver nanowires, *Carbohydr. Polym.*, 2016, **137**, 732–738.

120 N. Bosq, N. Guigo, L. Vincent and N. Sbirrazzuoli, Thermomechanical behavior of a novel biobased poly(furfurylalcohol)/silica nanocomposite elaborated by smart functionalization of silica nanoparticles, *Polym. Degrad. Stab.*, 2015, **118**, 137–146.

121 Y. L. Chung, S. Ansari, L. Estevez, S. Hayrapetyan, E. P. Giannelis and H. M. Lai, Preparation and properties of biodegradable starch–clay nanocomposites, *Carbohydr. Polym.*, 2010, **79**, 391–396.

122 H. M. Park, M. Misra, L. T. Drzal and A. K. Mohanty, "Green" Nanocomposites from Cellulose Acetate Bioplastic and Clay: Effect of Eco-Friendly Triethyl Citrate Plasticizer, *Biomacromolecules*, 2004, **5**, 2281–2288.

123 O. u. Rahman, M. Kashif and S. Ahmad, Nanoferrite dispersed waterborne epoxy-acrylate: anticorrosive nanocomposite coatings, *Prog. Org. Coat.*, 2015, **80**, 77–86.

124 M. M. Aung, W. J. Li and H. N. Lim, Improvement of Anticorrosion Coating Properties in Bio-Based Polymer Epoxy Acrylate Incorporated with Nano Zinc Oxide Particles, *Ind. Eng. Chem. Res.*, 2020, **59**, 1753–1763.

125 D. I. Njoku, M. Cui, H. Xiao, B. Shang and Y. Li, Understanding the anticorrosive protective mechanisms of modified epoxy coatings with improved barrier, active and self-healing functionalities: EIS and spectroscopic techniques, *Sci. Rep.*, 2017, **7**, 15597–15609.

126 M. C. Lai, K. C. Chang, J. M. Yeh, S. J. Liou, M. F. Hsieh and H. S. Chang, Advanced environmentally friendly anticorrosive materials prepared from water-based polyacrylate/Na^+-MMT clay nanocomposite latexes, *Eur. Polym. J.*, 2007, **43**, 4219–4228.

127 A. Saikia, D. Sarmah, A. Kumar and N. Karek, Bio-based epoxy/polyaniline nanofiber–carbon dot nanocomposites as advanced anticorrosive materials, *J. Appl. Polym. Sci.*, 2019, **136**, 47744–47755.

128 G. W. Curtzwiler, E. B. Williams, A. L. Maples, S. W. Wand and J. W. Rawlins, Measurable and Influential Parameters That Influence Corrosion Performance Differences between Multiwall Carbon Nanotube Coating Material Combinations and Model Parent Material Combinations Derived from Epoxy-Amine Matrix Materials, *ACS Appl. Mater. Interfaces*, 2017, **9**, 6356–6368.

129 G. W. Curtzwiler, E. B. Williams, A. L. Maples, S. W. Wand and J. W. Rawlins, Understanding the influence of water hydrogen bonding on the cathodic delamination rate of coated steel substrates from pre-exposure characterization, *Corros. Sci.*, 2019, **151**, 198–205.

130 D. Halder, A. Mitra, S. Bag, U. Raychaudhuri and R. Chakraborty, Study on Gelatin-Silver Nanoparticle Composite Towards the Development of Bio-Based Antimicrobial Film, *J. Nanosci. Nanotechnol.*, 2011, **12**, 10374–10378.

131 S. F. Hosseini, M. Rezaei, M. Zandi and F. Farahmandghavi, Development of bioactive fish gelatin/chitosan nanoparticles composite films with antimicrobial properties, *Food Chem.*, 2016, **194**, 1266–1274.

132 R. Jung, Y. Kim, H. S. Kim and H. J. Jin, Antimicrobial properties of hydrated cellulose membranes with silver nanoparticles, *J. Biomater. Sci., Polym. Ed.*, 2012, **20**, 311–324.

133 A. Fernandez, P. Picouet and E. Lloret, Cellulose–silver nanoparticle hybrid materials to control spoilage-related microflora in absorbent pads located in trays of fresh-cut melon, *Int. J. Food Microbiol.*, 2010, **142**, 222–228.

134 A. S. Abreu, M. Oliveira, A. d. Sa, R. M. Rodrigues, M. A. Cerqueria, A. A. Vicente and A. V. Machado, Antimicrobial nanostructured starch based films for packaging, Inhibition of microbial growth by silver–starch nanocomposite thin films, *Carbohydr. Polym.*, 2015, **129**, 127–134.

135 D. K. Božani, V. Djokovi, S. Dimitrijevi-Brankovi, R. Krsmanovi, M. McPherson, P. S. Nair, M. K. Georges and T. Radhakrishnan, Inhibition of microbial growth by silver–starch nanocomposite thin films, *J. Biomater. Sci., Polym. Ed.*, 2011, **22**, 2343–2355.

136 E. S. Abdel-Halim and S. S. Al-Deyab, Antimicrobial activity of silver/starch/polyacrylamide nanocomposite, *Int. J. Biol. Macromol.*, 2014, **68**, 33–38.

137 A. Usman, Z. Hussain, A. Riz and A. N. Khan, Enhanced mechanical, thermal and antimicrobial properties of poly(vinyl alcohol)/graphene oxide/starch/silver nanocomposites films, *Carbohydr. Polym.*, 2016, **153**, 592–599.

138 H. Barzegar, M. H. Azizi, M. Barzegar and Z. Hamidi-Esfahani, Effect of potassium sorbate on antimicrobial and physical properties of starch–clay nanocomposite films, *Carbohydr. Polym.*, 2014, **110**, 26–31.

139 J. Fu, J. Ji, D. Fan and J. Shen, Construction of antibacterial multilayer films containing nanosilver via layer-by-layer assembly of heparin and chitosan–silver ions complex, *J. Biomed. Mater. Res., Part A*, 2006, **79**, 665–674.

140 R. Tankhiwale and S. K. Bajpai, Silver-nanoparticle-loaded chitosan lactate films with fair antibacterial properties, *J. Appl. Polym. Sci.*, 2009, **115**, 1894–1900.

141 R. Yoksan and S. Chirachanchai, Silver nanoparticle-loaded chitosan–starch based films: fabrication and evaluation of tensile, barrier and antimicrobial properties, *Mater. Sci. Eng., C*, 2010, **30**, 891–897.

142 V. Thomas, M. M. Yallapu, B. Sreedhar and S. K. Bajpai, Fabrication, characterization of chitosan/nanosilver film and its potential antibacterial application, *J. Biomater. Sci., Polym. Ed.*, 2009, **20**, 2129–2144.

143 S. Murali, S. Kumar, J. Koh, S. Seena, P. Singh, A. Ramalho and A. J. F. N. Sobral, Bio-based chitosan/gelatin/Ag@ZnO bionanocomposites: synthesis and mechanical and antibacterial properties, *Cellulose*, 2019, **26**, 5347–5361.

144 W. K. Son, J. H. Youk and W. H. Park, Antimicrobial cellulose acetate nanofibers containing silver nanoparticles, *Carbohydr. Polym.*, 2006, **65**, 430–434.

145 S. Miao, Z. Miao, Z. Liu, B. Han, H. Zheng and J. Zhang, Synthesis of mesoporous TiO_2 films in ionic liquid dissolving cellulose, *Microporous Mesoporous Mater.*, 2006, **95**, 26–30.

146 V. Goudarzi, I. Shahabi-Ghahfarrokhi and A. Babaei-Ghazvini, Preparation of ecofriendly UV-protective food packaging material by starch/TiO_2 bio-nanocomposite: characterization, *Int. J. Biol. Macromol.*, 2017, **95**, 306–313.

147 S. A. Oleyaei, H. Almasi, B. Ghanbarzadeh and A. A. Moayedi, Synergistic reinforcing effect of TiO_2 and montmorillonite on potato starch nanocomposite films: thermal, mechanical and barrier properties, *Carbohydr. Polym.*, 2016, **152**, 253–262.

148 K. K. Gupta, P. K. Mishra, P. Srivastava, M. Gangwar, G. Nath and P. Maiti, Hydrothermal in situ preparation of TiO_2 particles onto poly(lactic acid) electrospun nanofibres, *Appl. Surf. Sci.*, 2013, **264**, 375–382.

149 J. Zeng, S. Liu, J. Cai and L. Zhang, TiO_2 Immobilized in Cellulose Matrix for Photocatalytic Degradation of Phenol under Weak UV Light Irradiation, *J. Phys. Chem. B*, 2010, **114**, 7806–7811.

150 Z. Hamden, S. Bouattour, A. M. Ferreira, D. P. Ferreira, L. F. V. Ferreira, A. M. B. d. Rego and S. Boufi, In situ generation of TiO_2 nanoparticles using chitosan as a template and their photocatalytic activity, *J. Photochem. Photobiol., A*, 2016, **321**, 211–222.

151 J. J. Zhou, S. Y. Wang and S. Gunasekaran, Preparation and Characterization of Whey Protein Film Incorporated with TiO_2 Nanoparticles, *J. Food Sci.*, 2009, **74**, N50–N56.

152 J. M. Feckl, A. Haynes, T. Bein and D. Fattakhova-Rohlfing, Thick titania films with hierarchical porosity assembled from ultrasmall titania nanoparticles as photoanodes for dye-sensitized solar cells, *New J. Chem.*, 2014, **38**, 1996–2001.

153 X. Lu and Y. Hu, Layer-by-layer Deposition of TiO_2 Nanoparticles in the Wood Surface and its Superhydrophobic Performance, *BioRes*, 2016, **11**, 4605–4620.

154 H. Pan, W. Wang, Y. Pan, W. Zeng, J. Zhan, L. Song, Y. Hu and K. M. Liew, Construction of layer-by-layer assembled chitosan/titanate nanotube based nanocoating on cotton fabrics: flame retardant performance and combustion behavior, *Cellulose*, 2015, **22**, 911–923.

155 S. Therias, J.-F. Larché, P.-O. Bussière, J.-L. Gardette, M. Murariu and P. Dubois, Photochemical Behavior of Polylactide/ZnO Nanocomposite Films, *Biomacromolecules*, 2012, **13**(10), 3283–3291.

156 S. Kumar, B. Krishnakumar, A. J. F. N. Sobral and J. Koh, Bio-based (chitosan/PVA/ZnO) nanocomposites film: Thermally stable and photoluminescence material for removal of organic dye, *Carbohydr. Polym.*, 2019, **205**, 559–564.

157 W. Li, L. Li, Y. Cao, T. Lan, H. Chen and Y. Qin, Effects of PLA Film Incorporated with ZnO Nanoparticle on the Quality Attributes of Fresh-Cut Apple, *Nanomaterials*, 2017, **7**(8), 207–227.

158 N. Vigneshwaran, S. Kumar, A. A. Kathe, P. V. Varadarajan and V. Prasad, Functional finishing of cotton fabrics using zinc oxide-soluble starch nanocomposites, *Nanotechnology*, 2006, **17**, 5087.

159 O. Carp, A. Tirsoaga, B. Jurca, R. Ene, S. Somacescu and A. Ianculescu, Biopolymer starch mediated synthetic route of multi-spheres and donut ZnO structures, *Carbohydr. Polym.*, 2015, **115**, 285–293.

160 K. Jradi, C. Maury and C. Daneault, Contribution of TEMPO-Oxidized Cellulose Gel in the Formation of Flower-Like Zinc Oxide Superstructures: Characterization of the TOC gel/ZnO Composite Films, *Appl. Sci.*, 2015, **5**, 1164–1183.

161 F. Cheng, J. W. Betts, S. M. Kelly, D. W. Wareham, A. Kornherr, F. Dumestre, J. Shaller and T. Heinze, Whiter, brighter, and more stable cellulose paper coated with antibacterial carboxymethyl starch stabilized ZnO nanoparticles, *J. Mater. Chem. B*, 2014, **2**, 3057–3064.

162 F. Fu, L. Li, L. Liu, J. Cai, Y. Zhang, J. Zhou and L. Zhang, Construction of Cellulose Based ZnO Nanocomposite Films with Antibacterial Properties through One-Step Coagulation, *ACS Appl. Mater. Interfaces*, 2015, **7**, 2597–2606.

163 Z. H. Ibupoto, K. Khun, M. Eriksson, M. A. Sahi, M. Atif, A. Ansari and M. Wilander, Hydrothermal Growth of Vertically Aligned ZnO Nanorods Using a Biocomposite Seed Later of ZnO Nanoparticles, *Materials*, 2013, **6**, 3584–3597.

164 H. Zhao and R. K. Y. Li, A study on the photo-degradation of zinc oxide (ZnO) filled polypropylene nanocomposites, *Polymer*, 2006, **47**(9), 3207–3217.

165 E. Olson, Y. Li, F. Y. Lin, A. Miller, F. Liu, A. Tsyrenova, D. Palm, G. Curtzwiler, K. Vorst, E. Cochran and S. Jiang, Thin Biobased Transparent UV-Blocking Coating Enabled by Nanoparticle Self-Assembly, *ACS Appl. Mater. Interfaces*, 2019, **11**, 24552–24559.

166 F. Fu, J. Gu, X. Xu, Q. Xiong, Y. Zhang, X. Liu and J. Zhou, Interfacial assembly of ZnO–cellulose nanocomposite films via a solution process: a one-step biomimetic approach and excellent photocatalytic properties, *Cellulose*, 2017, **24**, 147–162.

167 D. Valerini, L. Tammaro, F. Villani, A. Rizzo, I. Caputo, G. Paolella and G. Vigliotta, Antibacterial Al-doped ZnO coatings on PLA films, *J. Mater. Sci.*, 2020, **55**, 4830–4847.

168 F. S. Jebel and H. Almasi, Morphological, physical, antimicrobial and release properties of ZnO nanoparticles-loaded bacterial cellulose films, *Carbohydr. Polym.*, 2016, **149**, 8–19.

169 M. Hassannia-Kolaee, F. Khodaiyan, R. Pourahmad and I. Shahabi-Ghahfarrokhi, Development of ecofriendly bionanocomposite: whey protein isolate/pullulan films with nano-SiO_2, *Int. J. Biol. Macromol.*, 2016, **86**, 139–144.

170 T. Abitbol, A. Ahniyaz, R. Alvarez-Asencio, A. Fall and A. Swerin, Nanocellulose-Based Hybrid Materials for UV Blocking and Mechanically Robust Barriers, *ACS Appl. Bio Mater.*, 2020, **3**, 2245–2254.

171 J. Cai, S. Liu, J. Feng, S. Kimura, M. Wada, S. Kuga and L. Zhang, Cellulose–Silica Nanocomposite Aerogels by In Situ Formation of Silica in Cellulose Gel, *Angew. Chem., Int. Ed.*, 2012, **51**, 2076–2079.

172 R. J. B. Pinto, P. A. A. P. Marques, A. M. Barros-Timmons, T. Trindade and C. P. Neto, Novel SiO_2/cellulose nanocomposites obtained by in situ synthesis and via polyelectrolytes assembly, *Compos. Sci. Technol.*, 2008, **68**, 1088–1093.

173 N. Saxena, T. Naik and S. Paria, Organization of SiO_2 and TiO_2 Nanoparticles into Fractal Patterns on Glass Surface for the Generation of Superhydrophilicity, *J. Phys. Chem. C*, 2017, **121**, 2428–2436.

174 R. H. Hakim, J. Cailloux, O. O. Santana, J. Bou, M. Sanchez-Soto, J. Odent, J. M. Raquez, P. Dubois, F. Carrasco and M. L. Maspoch, PLA/SiO_2 composites: influence of the filler modifications on the morphology, crystallization behavior, and mechanical properties, *J. Appl. Polym. Sci.*, 2017, **134**, 45367.

175 F. Ai, H. Zheng, M. Wei and J. Huang, Soy protein plastics reinforced and toughened by SiO_2 nanoparticles, *J. Appl. Polym. Sci.*, 2007, **105**, 1597–1604.

176 B. Alonso and E. Belamie, Chitin–Silica Nanocomposite by Self-Assembly, *Angew. Chem., Int. Ed.*, 2010, **49**, 8201–8204.

177 E. D. H. Mansfield, Y. Pandya, E. A. Mun, S. E. Rogers, I. Abutbul-Ionita, D. Danino, A. C. Williams and V. V. Khutoryanskiy, Structure and characterisation of hydroxyethylcellulose–silica nanoparticles, *RSC Adv.*, 2018, **8**, 6471–6478.

178 M. Yadav, K. Y. Rhee, I. H. Jung and S. J. Park, Eco-friendly synthesis, characterization and properties of a sodium carboxymethyl cellulose/graphene oxide nanocomposite film, *Cellulose*, 2013, **20**, 687–698.

179 M. Tian, X. Hu, L. Qu, M. Du, S. Zhu, Y. Sun and G. Han, Ultraviolet protection cotton fabric achieved via layer-by-layer self-assembly of graphene oxide and chitosan, *Appl. Surf. Sci.*, 2016, **377**, 141–148.

180 H. Huang and X. Yang, Chitosan mediated assembly of gold nanoparticles multilayer, *Colloids Surf., A*, 2003, **226**, 77–86.

181 Z. Li, A. Fredrich and A. Taubert, Gold microcrystal synthesis via reduction of $HAuCl_4$ by cellulose in the ionic liquid 1-butyl-3-methylimidazolium chloride, *J. Mater. Chem.*, 2008, **18**, 1008–1014.

182 G. D. Carlo, A. Curulli, R. G. Toro, C. Bianchini, T. D. Caro, G. Padeletti, D. Zane and G. M. Ingo, Green Synthesis of Gold–Chitosan Nanocomposites for Caffeic Acid Sensing, *Langmuir*, 2012, **28**, 5471–5479.

183 Z. Liu, M. Li, L. Turyanska, O. Makarovsky, A. Patane, W. Wu and S. Mann, Self-Assembly of Electrically Conducting Biopolymer Thin Films by Cellulose Regeneration in Gold Nanoparticle Aqueous Dispersions, *Chem. Mater.*, 2010, **22**, 2675–2680.

184 T. K. Sarma and A. Cattopadhyay, Starch-Mediated Shape-Selective Synthesis of Au Nanoparticles with Tunable Longitudinal Plasmon Resonance, *Langmuir*, 2004, **20**, 3520–3524.

185 S. Padalkar, J. R. Capdona, S. J. Rowan, C. Weder, Y. H. Won, L. A. Stanciu and R. J. Moon, Natural Biopolymers: Novel Templates for the Synthesis of Nanostructures, *Langmuir*, 2010, **26**, 8497–8502.

186 Z. Cheng, Y. Ma, L. Yang, F. Cheng, Z. Huang, A. Natan, H. Li, Y. Chen, D. Cao, Z. Huang, Y. H. Wang, Y. Liu, R. Yang and H. Zhu, Plasmonic-Enhanced Cholesteric Films: Coassembling Anisotropic Gold Nanorods with Cellulose Nanocrystals, *Adv. Opt. Mater.*, 2019, **7**, 1801816.

187 C. T. Martins, C. S. R. Freire, R. J. B. Pinto, S. C. M. Fernandes, C. P. Neto, A. J. D. Silvestre, J. Causio, G. Baldi, P. Sadocco and T. Trindade, Electrostatic assembly of Ag nanoparticles onto nanofibrillated cellulose for antibacterial paper products, *Cellulose*, 2012, **19**, 1425–1436.

188 H. Liu, J. Song, S. Shang, Z. Song and D. Wang, Cellulose Nanocrystal/Silver Nanoparticle Composites as Bifunctional Nanofillers within Waterborne Polyurethane, *ACS Appl. Mater. Interfaces*, 2012, **4**, 2413–2419.

189 L. Liu, L. Wang, S. Luo, Y. Qing, N. Yan and Y. Wu, Chiral nematic assemblies of silver nanoparticles in cellulose nanocrystal membrane with tunable optical properties, *J. Mater. Sci.*, 2019, **54**, 6699–6708.

190 T. C. Mokhena and A. S. Luyt, Electrospun alginate nanofibres impregnated with silver nanoparticles: preparation, morphology and antibacterial properties, *Carbohydr. Polym.*, 2017, **165**, 304–312.

191 B. Tang, J. Wang, S. Xu, T. Afrin, J. Tao, W. Xu, L. Sun and X. Wang, Function improvement of wool fabric based on surface assembly of silica and silver nanoparticles, *Chem. Eng. J.*, 2012, **185**, 366–373.

192 T. W. Lee, S. E. Lee and Y. G. Jeong, Highly Effective Electromagnetic Interference Shielding Materials based on Silver Nanowire/Cellulose Papers, *ACS Appl. Mater. Interfaces*, 2016, **8**, 13123–13132.

193 S. Shankar, J. W. Rhim and K. Won, Preparation of poly(lactide)/lignin/silver nanoparticles composite films with UV light barrier and antibacterial properties, *Int. J. Biol. Macromol.*, 2018, **107**, 1724–1731.

194 L. T. T. Trinh, A. L. Kjoniksen, K. Zhu, K. D. Knudsen, S. Volden, W. R. Glomm and B. Nystom, Slow salt-induced aggregation of citrate-covered silver particles in aqueous solutions of cellulose derivatives, *Colloid Polym. Sci.*, 2009, **287**, 1391.

195 E. Fortunati, S. Mattioli, I. Armentano and J. M. Kenny, Spin coated cellulose nanocrystal/silver nanoparticle films, *Carbohydr. Polym.*, 2014, **113**, 394–402.

196 M. Basuny, I. O. Ali, A. A. El-Gawad, M. F. Bakr and T. M. Salama, A fast green synthesis of Ag nanoparticles in carboxymethyl cellulose (CMC) through UV irradiation technique for antibacterial applications, *J. Sol-Gel Sci. Technol.*, 2015, **75**, 530–540.

197 W. Xiao, J. Xu, X. Liu, O. Hu and J. Huang, Antibacterial hybrid materials fabricated by nanocoating of microfibril bundles of cellulose substance with titania/chitosan/silver-nanoparticle containing films, *J. Mater. Chem. B*, 2013, **1**, 3477–3485.

198 A. Gholoobi, Z. Meshkat, K. Abnous, M. Ghayour-Mobarhan, M. Ramezani, F. H. Shandiz, K. D. Verma and M. Darroudi, Biopolymer-mediated synthesis of Fe_3O_4 nanoparticles and investigation of their in vitro cytotoxicity effects, *J. Mol. Struct.*, 2017, **1141**, 594–599.

199 W. Yang, H. Tian, J. Liao, Y. Wang, L. Liu, L. Zhang and A. Lu, Flexible and strong Fe_3O_4/cellulose composite film as magnetic and UV sensor, *Appl. Surf. Sci.*, 2020, **507**, 145092.

200 K. Liu, J. Nasrallah, L. Chen, L. Huang and Y. Ni, Preparation of CNC-dispersed Fe_3O_4 nanoparticles and their application in conductive paper, *Carbohydr. Polym.*, 2015, **126**, 175–178.

201 J. Zhou, R. Li, S. Liu, Q. Li, L. Zhang, L. Zhang and J. Guan, Structure and magnetic properties of regenerated cellulose/Fe_3O_4 nanocomposite films, *J. Appl. Polym. Sci.*, 2008, **111**, 2477–2484.

202 A. Liu and L. A. Berglund, Clay nanopaper composites of nacre-like structure based on montmorillonite and cellulose nanofibers—improvements due to chitosan addition, *Carbohydr. Polym.*, 2012, **87**, 53–60.

203 S. Y. Yoon and Y. Deng, Clay–starch composites and their application in papermaking, *J. Appl. Polym. Sci.*, 2006, **100**, 1032–1038.

204 L. A. Castillo, O. V. Lopez, J. Ghilardi, M. A. Villar, S. E. Barbosa and M. A. Garcia, Thermoplastic starch/talc bionanocomposites. Influence of particle morphology on final properties, *Food Hydrocolloids*, 2015, **51**, 432–440.

205 S. S. Ray, R. Maiti, M. Okamoto, K. Tamada and K. Ueda, New Polylactide/Layered Silicate Nanocomposites. 1. Preparation, Characterization, and Properties, *Macromolecules*, 2002, **35**, 3104–3110.

206 K. Piekarska, P. Sowinski, E. Piorkowska, M. M.-U. Haque and M. Pracella, Structure and properties of hybrid PLA nanocomposites with inorganic nanofillers and cellulose fibers, *Composites, Part A*, 2016, **82**, 34–41.

207 A. Nuzzo, S. Coiai, S. C. Carroccio, N. T. Dintcheva, C. Gambarotti and G. Filippone, Heat-Resistant Fully Bio-Based Nanocomposite Blends Based on Poly(lactic acid), *Macromol. Mater. Eng.*, 2013, **299**, 31–40.

208 H. B. Yao, Z. H. Tan, H. Y. Fang and S. H. Yu, Artificial Nacre-like Bionanocomposite Films from the Self-Assembly of Chitosan–Montmorillonite Hybrid Building Blocks, *Angew. Chem., Int. Ed.*, 2010, **49**, 10127–10131.

209 C. Huang, X. Chen, Z. Xue and T. Wang, Effect of structure: a new insight into nanoparticle assemblies from inanimate to animate, *Sci. Adv.*, 2020, **6**, 1–13.

210 M. Yue, Y. Li, Y. Hou, W. Cao, J. Zhu, J. Han, Z. Lu and M. Yang, Hydrogen Bonding Stabilized Self-Assembly of Inorganic Nanoparticles: Mechanism and Collective Properties, *ACS Nano*, 2015, **9**, 5807–5817.

211 A. D. Buckingham, J. E. D. Bene and S. A. C. McDowell, The hydrogen bond, *Chem. Phys. Lett.*, 2008, **463**, 1–10.

212 B. Widom, P. Bhimalapuram and K. Koga, The hydrophobic effect, *Phys. Chem. Chem. Phys.*, 2003, **5**, 3085–3093.

213 M. A. Bevan and D. C. Prieve, Direct Measurement of Retarded van der Waals Attraction, *Langmuir*, 1999, **15**, 7925–7936.

214 E. Homede, A. Zigelman, L. Abezgauz and O. Manor, Signatures of van der Waals and Electrostatic Forces in the Deposition of Nanoparticle Assemblies, *J. Phys. Chem. Lett.*, 2018, **9**, 5226–5232.

215 H. Huang and E. Ruckenstein, The Bridging Force between Colloidal Particles in a Polyelectrolyte Solution, *Langmuir*, 2012, **28**, 16300–16305.

216 Y. N. Pandey, G. J. Papakonstantopoulos and M. Doxastakis, Polymer/Nanoparticle Interactions: Bridging the Gap, *Macromolecules*, 2013, **46**, 5097–5106.

217 S. Ji and J. Y. Walz, Depletion Flocculation Induced by Synergistic Effects of Nanoparticles and Polymers, *J. Phys. Chem. B*, 2013, **117**, 16602–16609.

218 H. Lekkerkerker and R. Tuinier, *Colloids and the Depletion Interaction*, Springer Netherlands, Hiedelberg, Germany, 2011, p. 234.

219 J. Walz and A. Sharma, Effect of Long Range Interactions on the Depletion Force between Colloidal Particles, *J. Colloid Interface Sci.*, 1994, **168**, 485–496.

220 D. Ray, V. K. Aswal and J. Kohlbrecher, Micelle-induced depletion interaction and resultant structure in charged colloidal nanoparticle system, *J. Appl. Phys.*, 2015, **117**(16), 164310.

221 M. Ahmed, Chapter 16 – Nanomaterial Synthesis, in *Polymer Science and Nanotechnology: Fundamentals and Applications*, ed. R. Narain, Elsevier, 2020.

222 B. Yuan, J. Zhang, Q. Mi, J. Yu, R. Song and J. Zhang, Transparent Cellulose–Silica Composite Aerogels with Excellent Flame Retardancy via an in Situ Sol–Gel Process, *ACS Sustainable Chem. Eng.*, 2017, **5**, 11117–11123.

223 K. E. Shopsowitz, H. Qi, W. Y. Hamad and M. J. MacLachlan, Free-standing mesoporous silica films with tunable chiral nematic structures, *Nature*, 2010, **468**, 422–425.

224 S. W. Zhao, M. Zheng, X. H. Zou, Y. Guo and Q. J. Pan, Self-Assembly of Hierarchically Structured Cellulose@ZnO Composite in Solid–Liquid Homogenous Phase: Synthesis, DFT Calculations, and Enhanced Antibacterial Activities, *ACS Sustainable Chem. Eng.*, 2017, **5**, 6585–6596.

225 Y. Liu, J. Wang, M. Zhang, H. Li and Z. Lin, Polymer-Ligated Nanocrystals Enabled by Nonlinear Block Copolymer Nanoreactors: Synthesis, Properties, and Applications, *ACS Nano*, 2020, **14**, 12491–12521.

226 A. Dong, J. Chen, X. Ye, J. M. Kikawa and C. B. Murray, Enhanced thermal stability and magnetic properties in NaCl-Type FePt–MnO binary nanocrystal superlattices, *J. Am. Chem. Soc.*, 2011, **133**, 13296–13299.

227 P. Podsiadlo, S. Paternel, J.-M. Rouillard, Z. Zhang, J. Lee, J.-W. Lee, E. Gulari and N. A. Kotov, Layer-by-layer assembly of nacre-like nanostructured composites with antimicrobial properties, *Langmuir*, 2005, **21**, 11915–11921.

228 A. G. Morena, I. Stefanov, K. Ivanova, S. Perez-Rafael, M. Sanches-Soto and T. Tzanov, Antibacterial polyurethane foams with incorporated lignin-capped silver nanoparticles for chronic wound treatment, *Ind. Eng. Chem. Res.*, 2020, **59**, 4504–4514.

229 Y. Chen, Z. Wang, Y. W. Harn, S. Pan, Z. Li, S. Lin, J. Peng, G. Zhang and Z. Lin, Resolving Optical and Catalytic Activities in ThermoresponsiveNanoparticles by Permanent Ligation with Temperature-SensitivePolymers, *Angew. Chem., Int. Ed.*, 2019, **58**, 11910–11917.

230 S. M. Yu, R. Wen, H. Y. Wang, Y. C. Zha, L. Qiu, B. Li, W. Xue and D. Ma, Chitosan-*graft*-Poly(L-lysine) Dendron-Assisted Facile Self-Assembly of Au Nanoclusters for Enhanced X-ray Computer Tomography Imaging and Precise MMP-9 Plasmid shRNA Delivery, *Chem. Mater.*, 2019, **31**, 3992–4007.

231 N. R. Neale and A. J. Frank, Size and shape control of nanocrystallites in mesoporous TiO_2 films, *J. Mater. Chem.*, 2007, **17**, 3216–3221.

232 P. Periyat, N. Leyland, D. E. McCormack, J. Colreavy, D. Corr and S. C. Pillai, Rapid microwave synthesis of mesoporous TiO_2 for electrochromic displays, *J. Mater. Chem.*, 2010, **20**, 3650–3655.

233 M. Barawi, L. D. Trizio, R. Giannuzzi, G. Veramonti, L. Manna and M. Manca, Dual Band Electrochromic Devices Based on Nb-Doped TiO_2 Nanocrystalline Electrodes, *ACS Nano*, 2017, **11**, 3576–3584.

234 R. Giannuzzi, T. Prontera, D. M. Tobaldi, M. Pugliese, L. D. Marco, S. Carallo, G. Gigli, R. C. Pullar and V. Maiorano, Pseudocapacitive behaviour in sol–gel derived electrochromic titania nanostructures, *Nanotechnology*, 2021, **32**, 045703.

235 W. Chen, J. Zhang, Q. Fang, S. Li, J. Wu, F. Li and K. Jiang, Sol–gel preparation of thick titania coatings aided by organic binder materials, *Sens. Actuators, B*, 2004, **100**, 195–199.

236 A. M. Bakhshayesh and M. R. Mohammadi, Development of nanostructured porous TiO_2 thick film with uniform spherical particles by a new polymeric gel process for dye-sensitized solar cell applications, *Electrochim. Acta*, 2013, **89**, 90–97.

237 J. W. Gilman, T. Kashiwagi and J. D. Lichtenhan, Nanocomposites: a revolutionary new flame retardant approach, *SAMPE J.*, 1997, **33**, 40–46.

238 D. W. Lee and B. R. Yoo, Advanced silica/polymer composites: materials and applications, *J. Ind. Eng. Chem.*, 2016, **38**, 1–12.

239 E. Olson, J. Blisko, C. Du, Y. Liu, Y. Li, H. Thurber, G. Curtzwiler, J. Ren, M. Thuo, X. Yong and S. Jiang, Biobased Superhydrophobic Coating Enabled by Nanoparticle Assembly, *Nanoscale Adv.*, 2021, Advance Article.

240 B. Zhang, S. A. Davis and S. Mann, Starch Gel Templating of Spongelike Macroporous Silicalite Monoliths and Mesoporous Films, *Chem. Mater.*, 2002, **14**, 1369–1375.

241 K. Majeed, M. Jawaid, A. Hassan, A. A. Bakar, H. P. S. A. Khalil, A. A. Salema and I. Inuwa, Potential materials for food packaging from nanoclay/natural fibres filled hybrid composites, *Mater. Des.*, 2013, **46**, 391–410.

242 D. A. P. d. Abreu, P. P. Losada, I. Ingulo and J. M. Cruz, Development of new polyolefin films with nanoclays for application in food packaging, *Eur. Polym. J.*, 2007, **43**, 2229–2243.

243 C. Tang, N. Chen, Q. Zhang, Q. Fu and X. Zhang, Preparation and properties of chitosan nanocomposites with nanofillers of different dimensions, *Polym. Degrad. Stab.*, 2009, **94**, 124–131.

244 A. Giannakas, M. Vlancha, C. Salmas, A. Leontiou, P. Katapodis, H. Stamatis, N.-M. Barkoula and A. Ladavos, Preparation, characterization, mechanical, barrier and antimicrobial properties of chitosan/PVOH/clay nanocomposites, *Carbohydr. Polym.*, 2016, **140**, 408–415.

245 G. Cavallaro, G. Lazzara and S. Milioto, Dispersions of Nanoclays of Different Shapes into Aqueous and Solid Biopolymeric Matrices. Extended Physicochemical Study, *Langmuir*, 2011, **27**, 1158–1167.

246 H. T. Ong, N. M. Julkapli, S. B. A. Hamid, O. Boondamnoen and M. F. Tai, Effect of magnetic and thermal properties of

iron oxide nanoparticles (IONs) in nitrile butadiene rubber (NBR) latex, *J. Magn. Magn. Mater.*, 2015, **395**, 173–179.

247 R. J. B. Pinto, P. A. A. P. Marques, M. A. Martins, C. P. Neto and T. Trindade, Electrostatic assembly and growth of gold nanoparticles in cellulosic fibres, *J. Colloid Interface Sci.*, 2007, **312**, 506–512.

248 Q. Liu, M. G. Campbell, J. S. Evans and I. I. Smalyukh, Orientationally Ordered Colloidal Co-Dispersions of Gold Nanorods and Cellulose Nanocrystals, *Adv. Mater.*, 2014, **26**, 7178–7184.

249 G. G. Vogiatzis and D. N. Theodorou, Multiscale Molecular Simulations of Polymer-Matrix Nanocomposites, *Arch. Comput. Methods Eng.*, 2018, **25**, 591–645.

250 A. Karatrantos, N. Clarke and M. Kroger, Modeling of Polymer Structure and Conformations in Polymer Nanocomposites from Atomistic to Mesoscale: A Review, *Polym. Rev.*, 2016, **56**, 385–428.

251 V. Ganesan and A. Jayaraman, Theory and simulation studies of effective interactions, phase behavior and morphology in polymer nanocomposites, *Soft Matter*, 2014, **10**, 13–38.

252 L.-T. Yan and X.-M. Xie, Computational modeling and simulation of nanoparticle self-assembly in polymeric systems: Structures, properties and external field effects, *Prog. Polym. Sci.*, 2013, **38**, 369–405.

253 V. Ganesan, Some issues in polymer nanocomposites: Theoretical and modeling opportunities for polymer physics, *J. Polym. Sci., Part B: Polym. Phys.*, 2008, **46**, 2666–2671.

254 G. Allegra, G. Raos and M. Vacatello, Theories and simulations of polymer-based nanocomposites: From chain statistics to reinforcement, *Prog. Polym. Sci.*, 2008, **33**, 683–731.

255 Q. H. Zeng, A. B. Yu and G. Q. Lu, Multiscale modeling and simulation of polymer nanocomposites, *Prog. Polym. Sci.*, 2008, **33**, 191–269.

256 L. M. Hall, A. Jayaraman and K. S. Schweizer, Molecular theories of polymer nanocomposites, *Curr. Opin. Solid State Mater. Sci.*, 2010, **14**, 38–48.

257 J. Liu, Y. Gao, D. Cao, L. Zhang and Z. Guo, Nanoparticle Dispersion and Aggregation in Polymer Nanocomposites: Insights from Molecular Dynamics Simulation, *Langmuir*, 2011, **27**, 7926–7933.

258 M. Gervasio and K. Lu, Monte Carlo Simulation Modeling of Nanoparticle–Polymer Cosuspensions, *Langmuir*, 2019, **35**, 161–170.

259 S. Lu, Z. Wu and A. Jayaraman, Molecular Modeling and Simulation of Polymer Nanocomposites with Nanorod Fillers, *J. Phys. Chem. B*, 2021, **125**, 2435–2449.

260 R. R. Faria, R. F. Guerra, L. R. d. S. Neto, L. F. Motta and E. d. F. Franca, Computational study of polymorphic structures of α- and β- chitin and chitosan in aqueous solution, *J. Mol. Graphics*, 2016, **63**, 78–84.

261 M. Petrov, L. Lymperakis, M. Friak and J. Neugebauer, Ab Initio Based conformational study of the crystalline α-chitin, *Biopolymers*, 2012, **99**, 22–34.

262 Z. Yu and D. Lau, Molecular dynamics study on stiffness and ductility in chitin–protein composite, *J. Mater. Sci.*, 2015, **50**, 7149–7157.

263 Z. Střelcová, P. Kulhánek, M. Friák, H.-O. Fabritius, M. Petrov, J. Neugebauer and J. Koča, The structure and dynamics of chitin nanofibrils in an aqueous environment revealed by molecular dynamics simulations, *RSC Adv.*, 2016, **6**, 30710–30721.

264 A. Kawska, O. Hochrein, J. Brickmann, R. Kniep and D. Zahn, The Nucleation Mechanism of Fluorapatite–Collagen Composites: Ion Association and Motif Control by Collagen Proteins, *Angew. Chem., Int. Ed.*, 2008, **47**, 4982–4985.

265 A. K. Nair, A. Gautieri, S.-W. Chang and M. J. Buehler, Molecular mechanics of mineralized collagen fibrils in bone, *Nat. Commun.*, 2013, **4**, 1724.

266 F. Jabeen, M. I. Arshad, K. M. Zia, M. S. U. Hasan, M. Younas, M. Akhtar and A. U. Rehman, Chapter 15 – computational modeling for bionanocomposites, in *Micro and Nano Technologies, Bionanocomposites*, ed. K. M. Zia, F. Jabeen, M. N. Anjum and S. Ikram, Elsevier, Amsterdam, Netherlands, 2020, pp. 367–420.

267 J. H. Harding and D. M. Duffy, The challenge of biominerals to simulations, *J. Mater. Chem.*, 2006, **16**, 1105–1112.

268 P. Kumar, K. P. Sandeep, S. Alavi and V. D. Truong, A Review of Experimental and Modeling Techniques to Determine Properties of Biopolymer-Based Nanocomposites, *J. Food Sci.*, 2010, **76**, E2–E14.

269 D. Zahn, Multi-scale simulations of apatite–collagen composites: from molecules to materials, *Front. Mater. Sci.*, 2017, **11**, 1–12.

270 C. P. Okoli, Q. J. Guo and G. O. Adewuyi, Application of quantum descriptors for predicting adsorption performance of starch and cyclodextrin adsorbents, *Carbohydr. Polym.*, 2014, **101**, 40–49.

271 D. Zahn, O. Hochrein, A. Kawska, J. Brickmann and R. Kniep, Towards an atomistic understanding of apatite–collagen biomaterials: linking molecular simulation studies of complex-, crystal- and composite-formation to experimental findings, *J. Mater. Sci.*, 2007, **42**, 8966–8973.

272 N. Almora-Barrios and N. H. D. Leeuw, Molecular Dynamics Simulation of the Early Stages of Nucleation of Hydroxyapatite at a Collagen Template, *Cryst. Growth Des.*, 2012, **12**, 756–763.

273 M. Cutini, M. Corno, D. Costa and P. Ugliengo, How Does Collagen Adsorb on Hydroxyapatite? Insights From Ab Initio Simulations on a Polyproline Type II Model, *J. Phys. Chem. C*, 2019, **123**, 7540–7550.

274 F. Peng, F. Pan, H. Sun, L. Lu and Z. Jiang, Novel nanocomposite pervaporation membranes composed of poly(vinyl alcohol) and chitosan-wrapped carbon nanotube, *J. Membr. Sci.*, 2007, **300**, 13–19.

275 S. Ebrahimi, K. Ghafoori-Tabrizi and H. Rafii-Tabar, Multi-scale computational modelling of the mechanical behaviour of the chitosan biological polymer embedded

with graphene and carbon nanotube, *Comput. Mater. Sci.*, 2012, **53**, 347–353.

276 S. Ebrahimi and H. Rafii-Tabar, Influence of hydrogen functionalization on mechanical properties of graphene and CNT reinforced in chitosan biological polymer: multi-scale computational modelling, *Comput. Mater. Sci.*, 2015, **101**, 189–193.

277 D. Aztazi-Pluma, E. O. Castrejon-Gonzalez, A. Almendarez-Camarillo, J. F. J. Alvarado and Y. Duran-Morales, Study of the Molecular Interactions between Functionalized Carbon Nanotubes and Chitosan, *J. Phys. Chem. C*, 2016, **120**, 2371–2378.

278 B. Ji and H. Gao, A study of fracture mechanisms in biological nano-composites via the virtual internal bond model, *Mater. Sci. Eng., A*, 2004, **366**, 96–103.

279 B. Ji and H. Gao, Mechanical Principles of Biological Nanocomposites, *Annu. Rev. Mater. Res.*, 2010, **40**, 77–100.

280 F. Chivrac, O. Gueguen, E. Pollet, S. Ahzi, A. Makradi and L. Averous, Micromechanical modeling and characterization of the effective properties in starch-based nano-biocomposites, *Acta Biomater.*, 2008, **4**, 1707–1714.

281 M. Raj, S. P. Patil and B. Markert, Mechanical Properties of Nacre-Like Composites: A Bottom-Up Approach, *J. Compos. Sci.*, 2020, **4**, 35.

282 X. Wei, M. Naraghi and H. D. Espinosa, Optimal Length Scales Emerging from Shear Load Transfer in Natural Materials: Application to Carbon-Based Nanocomposite Design, *ACS Nano*, 2012, **6**, 2333–2344.

283 M. J. Snowden, S. M. Clegg, P. A. Williams and I. D. Robb, Flocculation of silica particles by adsorbing and non-adsorbing polymers, *J. Chem. Soc., Faraday Trans.*, 1991, **87**, 2201–2207.

284 S. Jungblut, J.-O. Joswig and A. Eychmuller, Diffusion-Limited Cluster Aggregation: Impact of Rotational Diffusion, *J. Phys. Chem. C*, 2019, **123**, 950–954.

285 S. Jungblut, J.-O. Joswig and A. Eychmuller, Diffusion- and reaction-limited cluster aggregation revisited, *Phys. Chem. Chem. Phys.*, 2019, **21**, 5723–5729.